NACA RM E52G08

NACA

RESEARCH MEMORANDUM

PERFORMANCE CHARACTERISTICS AT MACH NUMBERS TO 2.0 OF VARIOUS TYPES OF SIDE INLETS MOUNTED ON FUSELAGE OF PROPOSED SUPERSONIC AIRPLANE

II - INLETS UTILIZING HALF OF A CONICAL SPIKE

By J. L. Allen and P. C. Simon

Lewis Flight Propulsion Laboratory
Cleveland, Ohio

NATIONAL ADVISORY COMMITTEE
FOR AERONAUTICS

WASHINGTON
September 4, 1952

NATIONAL ADVISORY COMMITTEE FOR AERONAUTICS

RESEARCH MEMORANDUM

PERFORMANCE CHARACTERISTICS AT MACH NUMBERS TO 2.0 OF VARIOUS TYPES OF SIDE INLETS MOUNTED ON FUSELAGE OF PROPOSED SUPERSONIC AIRPLANE

II - INLETS UTILIZING HALF OF A CONICAL SPIKE

By J. L. Allen and P. C. Simon

SUMMARY

An investigation was made to determine the performance of twin-scoop side inlets mounted on the fuselage of a proposed supersonic aircraft. The inlets utilized half of a conical spike as the compression surface and a ram-type boundary-layer-removal system. Two types of splitter plates were used to separate the flow entering the boundary-layer duct and main inlet. Also, two longitudinal positions of the semicone were tested to simulate a variable-geometry inlet. This research was conducted at the NACA Lewis 8- by 6-foot supersonic tunnel at Mach numbers of 0.63 and 1.5 to 2.0 at angles of attack from 0° to 12°. Tests were also made at zero flight Mach number to evaluate take-off performance.

Peak total-pressure recoveries of about 0.86 to 0.95 were obtained at flight Mach numbers of 2.0 and 1.5, respectively, at the intended cruise angle of attack of 3° with complete removal of the fuselage boundary layer forward of the inlet. The Mach number of the flow immediately ahead of the inlet was about 1.83 at a flight Mach number of 2.0 and about 1.39 at a flight Mach number of 1.5. The inlet captured practically all the local stream tube at a flight Mach number of 2.0 and at a critical pressure recovery of 0.83.

At a flight Mach number of 1.5, translating the semicone to the aft position increased the captured mass flow with no significant change in pressure recovery. However, at flight Mach numbers of 1.9 and 2.0 with the cone in the aft position, the operating range of the inlet was severely limited by pulsing, and pressure recovery was substantially reduced.

Peak total-pressure recovery varied from 0.88 to 0.70 for angles of attack from 0° to 12° at a flight Mach number of 2.0. At a flight Mach number of 1.5, pressure recovery did not change appreciably as the

angle of attack varied from 0° to 9°. Sweeping back the splitter-plate leading edge increased the stable subcritical operating range of the inlet at a flight Mach number of 2.0 for angles of attack from 0° to 9°.

At the subsonic Mach number of 0.63 a pressure recovery of 0.97 was attained for critical inlet flow with the cone in the aft position. At zero forward velocity a large vena-contracta effect was observed which may limit the performance at take-off unless auxiliary inlets are used.

INTRODUCTION

The performance of scoop or side-type inlets is not as well known as that of symmetrical nose inlets. Previous preliminary investigations of half-cone inlets reported in references 1 and 2 simulated a fuselage inlet installation by utilizing flat plates to generate boundary layer ahead of the inlets. For these investigations, uniform supersonic flow fields were maintained ahead of the inlets, and pressure recoveries comparable with conical nose inlets were obtained when the boundary layer was completely removed. In the practical application of an inlet to an airplane, the entire flow field at the inlet can be distorted because of asymmetrical body shape and body cross-flow effects at angle of attack, possibly causing detrimental effects on performance. An investigation of the performance of several types of scoop inlets located on a supersonic aircraft fuselage has been conducted in the NACA Lewis 8- by 6-foot supersonic tunnel. Only one location of the inlets on the body has been considered. A general comparison of the over-all performance of various types of inlets is presented in reference 3. This report presents detailed performance data of an investigation of half-cone-type inlets. Detailed results for ramp-type inlets are presented in reference 4.

The investigation was conducted over a range of supersonic Mach numbers from 1.5 to 2.0 and at subsonic Mach numbers of 0 and 0.63 at angles of attack from 0° to 12°. Two longitudinal positions of the semicone were investigated as well as various inlet modifications.

SYMBOLS

The following symbols are used in this report:

A	area
C_D	model external drag coefficient based on maximum fuselage cross-sectional area of 1.784 sq ft
h	height above canopy of boundary-layer-scoop leading edge, in.
M	Mach number

[redacted]

m	mass flow
P	total pressure
p	static pressure
V	velocity
y	normal distance from splitter plate or radial distance from cone at plane of survey, in.
α	angle of attack
β	inlet flow approach angle
δ	boundary-layer thickness, in.
ρ	mass density of air

Subscripts:

b	distinguishes boundary-layer mass-flow ratios from those of main inlet
c	canopy
d	boundary-layer duct
p	projected, mass flow based on projected inlet area normal to canopy
l	left wedge bar
max	maximum
r	right wedge bar
s	boundary-layer scoop
0	free stream
1	minimum inlet area
1'	inlet-entrance rake station, model station 73.0
2	diffuser-discharge rake station, model station 97.25

[redacted]

Pertinent mass-flow ratios:

$\frac{m_2}{m_{0,p}}$ $\frac{\text{mass flow through inlet}}{\rho_0 V_0 A_p}$

$\frac{m_2}{m_{0,1}}$ $\frac{\text{mass flow through inlet}}{\rho_0 V_0 A_1}$

$\frac{m_2}{m_{max}}$ $\frac{\text{mass flow through inlet}}{\text{maximum theoretical mass flow for choking at minimum area}}$

$\left(\frac{m_s}{m_c}\right)_b$ boundary-layer-scoop mass-flow ratio = $\frac{\text{mass flow entering at scoop leading edge}}{\text{mass flow available at canopy for given scoop height}}$

$\left(\frac{m_d}{m_0}\right)_b$ $\frac{\text{boundary-layer-duct mass flow}}{\rho_0 V_0 A_d}$

APPARATUS AND PROCEDURE

A photograph of the quarter-scale model investigated showing half-cone inlets installed on the fuselage forebody of a proposed aircraft is presented in figure 1. Plan and side views, including typical cross sections of the basic fuselage, are shown in figure 2. Schematic cross sections of the various inlets investigated (sections are taken at the inlet center line in a plane normal to the fuselage) are presented in figure 3, and the resultant area distributions of the diffusers are shown in figure 4. The longitudinal center lines of the inlet cones were parallel to the angle-of-attack axis. The inlets were halves of external compression single-conical shock inlets with a subsonic-duct transition from a semicircular entrance to a circular passage; the duct discharge was approximately 5.3 inlet diameters aft and 0.1 inlet diameter down relative to the tip of the half cone. Typical cross sections of the subsonic duct are indicated in figure 4. A splitter plate separated the flow entering the inlet and that entering the ram-type boundary-layer scoop and extended across the full width of the inlet. The internal boundary-layer duct made a constant-area transition into a circular duct which discharged parallel to the main airflow ducts.

The first inlet investigated (fig. 3(a)) had a semicone angle of 25°. The tip of the cone was positioned for conical shock

intersection with the cowl lip at a local Mach number of approximately 2.0. The top plane of the splitter plate was parallel to the fuselage axis. The boundary-layer scoops had enclosed sides and were 0.44 inch high at the entrance. Three accumulative modifications were evaluated on the first inlet: (1) The sides of the boundary-layer scoops were removed to the plane of the inlet, (2) the canopy lines (canopy refers to the flat surface immediately forward of the inlet) were modified as shown in figure 3(a) to provide a boundary-layer scoop height of 0.80 inch, and (3) a slot $2\frac{1}{8}$ inches long by 1/2' inch high was cut in each side of the inlet cowling adjacent to the inlet floor.

2507

The second inlet (figs. 3(b) and 3(c)), hereinafter called the redesigned inlet, was installed with the splitter-plate surface parallel to the unmodified canopy. The semicone angle was again 25°, but the initial tip position was selected to give conical shock interception with the cowl lip at a local canopy Mach number of 1.83 (corresponding to a flight Mach number of 2.0). In order to attain a boundary-layer scoop height of 0.80 inch, the splitter plate, cone, and cowling were moved forward so that external lines could be faired into existing fuselage lines at station 79.5. The sides of the boundary-layer scoop were eliminated as far as $1\frac{1}{2}$ inches aft of the cowl lip. A second longitudinal position of the semicone, 0.93 inch aft of the splitter-plate leading edge, was also investigated.

In figure 5 is shown a photograph of typical inlet and removable canopy instrumentation installed on the starboard (pilot's right) inlet of one of the modifications of the first configuration. Instrumentation, testing technique, and data reduction methods are similar to those of reference 4. A mean total pressure at the inlet-entrance rake plane of survey was obtained by an area weighting of the rake profiles. Thirteen sets of total-pressure tubes (1/4 in. from the inlet floor) and static-orifice taps were located in three longitudinal rows to determine if separated flow existed in the subsonic diffuser.

Mass flows were computed for choking at the control plug with the use of an average (area weighting) total pressure at the diffuser exit rake for supersonic and zero flight Mach numbers. Diffuser-discharge Mach numbers were computed from the one-dimensional area ratio relation between the sonic discharge and rake stations. At a flight Mach number of 0.63, the control plug was not choked, and therefore diffuser-discharge Mach numbers were computed from mass-flow and total-pressure measurements to satisfy one-dimensional continuity relations. Mass-flow ratio for the supersonic Mach numbers is based on the inlet projected area normal to the canopy, which was 16.9 square inches for the first inlet and 13.3 square inches for the redesigned inlet. Mass-flow ratios for flight Mach numbers of 0.63 and zero are based on minimum inlet flow area.

Two mass-flow ratios are used to describe the flow of the boundary-layer air. The ratio of mass flow entering the scoop to that available at the canopy measuring station for a given scoop height is defined as the scoop mass-flow ratio $(m_s/m_c)_b$. The boundary-layer-duct mass-flow ratio $(m_d/m_0)_b$ is the ratio of duct mass flow to that of a free-stream tube with area equal to the duct area (constant-area duct). The latter ratio is considered more accurate than the scoop mass flow inasmuch as it does not depend on canopy measurements.

Drag force is defined as thrust (change in momentum of the air flow through the main inlets from free stream to diffuser rake station) minus the summation of strain-gage balance forces and base force. Forces on the mass-flow control plugs were not measured by the balance. The momentum decrement associated with the flow in the boundary-layer ducts is included in the drag force.

2507

Data for the simulated static conditions were obtained by attaching exhauster equipment to the model discharge ducts. Reynolds number based on fuselage length forward of the inlets was approximately 29×10^6 at supersonic Mach numbers and 19×10^6 at a flight Mach number of 0.63.

RESULTS AND DISCUSSION

First Inlet

The variation of inlet mass-flow ratio and total-pressure recovery with diffuser-discharge Mach number for the cruise angle of attack of 3° and a flight Mach number of 2.0 is shown in figure 6 for the first inlet. The boundary-layer-scoop mass-flow ratio was intended to approximately satisfy aircraft cooling requirements. The inlet mass-flow ratio is based on free-stream density and velocity and projected inlet area at the canopy.

The peak pressure recovery of 0.66 obtained is comparatively low inasmuch as recovery for a normal shock at a Mach number of 2.0 is 0.72. The low recovery can be primarily attributed to boundary-layer air entering the inlet. This is substantiated by the canopy flow surveys reported in reference 4, which indicated that the boundary-layer thickness ahead of the inlet for the same fuselage was 0.80 inch or an h/δ of 0.55 for a scoop height of 0.44 inch. Furthermore, the boundary-layer scoop is operating subcritically as evidenced by the scoop mass-flow ratio of only 0.38. The schlieren photograph in figure 7 depicts boundary-layer air entering the inlet and subcritical scoop operation. In addition, inclination of the splitter plate relative to the local

flow direction causes an expansion ahead of the inlet which accelerates the flow, in this case from a local canopy Mach number of 1.83 to a Mach number of the order of 2.0 to 2.1. Consequently, the losses through the inlet shock system are greater than would be attained for an inlet alined with the local flow, which would utilize the favorable compression from the forebody and canopy.

By eliminating the sides of the boundary-layer scoop, critical operation (no spillage) was attained at the scoop leading edge. This modification increased the peak pressure recovery from 0.66 obtained with enclosed scoop sides to 0.71 for respective scoop mass-flow ratios of 0.38 and 1.0, as shown in figure 8(a). The maximum mass-flow ratio of the inlet was increased from about 0.90 to 0.94. This result agrees qualitatively with the effects of h/δ and scoop mass-flow ratio presented in reference 1.

Provisions for varying the scoop height were not provided; therefore, the canopy surface was modified to attain the desired scoop height of 0.80 inch, as shown by the dashed line in figure 3(a). Data for this modification, shown in figure 8(b), indicate a peak pressure recovery of 0.73 compared with the value of 0.71 obtained with $h/\delta = 0.55$ and scoop sides eliminated. This result is much smaller than would be anticipated from reference 1, thus indicating that the modification was relatively unsuccessful. It is believed that modifying the canopy possibly increased the boundary-layer thickness and the static-pressure gradient at the inlet; each has an adverse effect on inlet performance. The resulting change of the inlet flow field is indicated by comparing the schlieren photographs presented in figure 9.

The third modification was to cut longitudinal slots in the inlet cowling, similar to the method used in reference 1, so that low-energy air could spill out the sides. Spilling air out the slots increased the peak pressure recovery from 0.73 to 0.75 (fig. 10), which is still considerably less than that of comparable nose inlets. The mass-flow ratio, at peak pressure recovery, was reduced from 0.94 (see fig. 8(b)) to 0.85. Inasmuch as the desired modifications could not be accomplished because of physical model limitations, the canopy fairing was restored to the original shape and the inlet was completely redesigned.

Redesigned Inlet

Surveys of the flow field of the unmodified canopy indicated practically no loss of free-stream total pressure outside of the boundary layer (reference 4); thus the efficient compression afforded by the forebody and pilot's canopy can be utilized by alining the splitter plate with the canopy surface and eliminating acceleration of the flow.

Analysis of schlieren photographs and data from the canopy-pitot-tube and flow-deflection-wedge instrumentation at an angle of attack of 3° indicated the following average canopy Mach numbers:

Flight Mach number, M_O	Canopy Mach number, M_c
1.5	1.39
1.7	1.57
1.9	1.74
2.0	1.83

2507

In addition to alining the redesigned inlet with the canopy, the following changes were made:

(1) Boundary-layer-scoop height was 0.8 inch or $h/\delta = 1.0$ at $\alpha = 3^\circ$.

(2) The cowling lip was moved forward to intercept the conical shock at a local Mach number of 1.83 (flight Mach number of 2.0).

(3) Sides of the boundary-layer scoop were eliminated and cut out further aft to reduce the possibility of spilled air entering the inlet.

Although the inlet was effectively yawed about $3\frac{1}{2}^\circ$ because of body cross flow at an angle of 3° (see Performance of the redesigned inlet at angle of attack), it was not possible to modify the inlets to minimize the effects of cross flow.

In order to summarize the effect of these changes, performance characteristics of the redesigned inlet are compared in figure 11 with the first inlet with scoop sides eliminated (data from fig. 8(a)) at the design flight Mach number of 2.0 and the cruise angle of attack of 3°. A peak pressure recovery of about 0.86 was obtained for the redesigned inlet, which is comparable with the performance of well-designed ramp-type side inlets (reference 4). The pressure recovery for critical flow was 0.83. A comparison of the respective supercritical drag coefficients (based on maximum fuselage cross-sectional area) indicates a 28 percent reduction for the redesigned inlet; this is primarily caused by the reduction in additive drag associated with decreasing the inlet air spillage from approximately 18 to less than 1 percent of the mass flow of a local stream tube determined by the canopy flow survey. Low-mass-flow spillage in the supercritical region and complete removal of the boundary layer are shown qualitatively by the schlieren photograph in figure 12. The redesigned inlet had a stable subcritical operating range of about 12 percent of the critical mass flow.

Varying the boundary-layer-duct mass-flow ratio changed the spillage out the sides of the scoop but did not change the scoop mass-flow ratio or significantly alter the mass flow entering the inlet.

Performance of redesigned inlet at various flight Mach numbers and cruise angle of attack of 3°. - In order to simulate variable-geometry inlets, the performance of the redesigned half-conical spike inlet was investigated over a range of supersonic flight Mach numbers for two longitudinal cone positions. The variation of mass-flow ratio, total-pressure recovery, and external drag coefficient with diffuser-discharge Mach number is presented in figure 13 for two longitudinal cone positions.

Pressure recoveries from 0.95 to 0.86 were obtained over the range of flight Mach numbers from 1.5 to 2.0 (see fig. 13(a)) with the cone in the forward, or estimated $M_0 = 2.0$, design position. At a flight Mach number of 1.5, the inlet is capturing approximately 88 percent of a stream tube evaluated at the local canopy conditions.

At a flight Mach number of 1.5, shifting the semicone to the aft position did not significantly change the pressure recovery. Captured mass flow increased to 93 percent of a local stream tube because the conical shock moved closer to the cowl lip and thus reduced spillage. Concomitantly, the drag coefficient for critical flow decreased slightly. The 7-percent spillage for the aft cone position probably could not be appreciably reduced by moving the cone further aft because of the slight internal contraction of the inlet.

At flight Mach numbers of 1.9 and 2.0, the stable subcritical operating range was considerably reduced compared with that obtained with the cone in the forward position. Translating the cone aft substantially reduced the peak pressure recoveries from about 0.86 (forward cone) to 0.81 with a 16 percent increase in mass flow at a flight Mach number of 2.0 and from 0.90 (forward cone) to 0.86 with a 23 percent increase in mass flow at a flight Mach number of 1.9.

The effect of translating the cone is primarily of interest when the breathing characteristics of turbojet engines are considered; as an example, the inlet-engine matching line for engine B of reference 5 at an altitude of 35,000 feet is indicated in figure 13. Translating the cone enables the engine air-flow requirements to be satisfied at more efficient diffuser points, that is, nearer to peak pressure recovery and minimum drag.

The theoretical conical and normal shock recovery for a 25° half-angle cone at a Mach number of 1.83 is about 0.95 compared with 0.83 (critical) experimentally obtained herein. To determine if the

disagreement is associated with the external or internal flow, total-pressure losses from free-stream conditions to the inlet entrance-rake measuring station, and from the inlet rakes to the diffuser exit for the two cone positions over the range of flight Mach numbers, were plotted (fig. 14) as a function of diffuser-discharge Mach number. Since the inlet rake station is about 3½ inches aft of the cowling lip, the $\Delta P_{0-1'}/P_0$ losses include the internal losses from the cowl lip to the rake; however, these are believed to be comparatively small. The internal duct losses $\Delta P_{1'-2}/P_0$ are practically independent of flight Mach number and primarily dependent on mass flow and velocity in the diffuser. Over what could be considered the useful operating range of the diffuser, the losses vary in the subcritical range from about 1 to 4 percent of the free-stream total pressure.

The inlet losses $\Delta P_{0-1'}/P_0$ are primarily dependent on flight Mach number and on shock structure as determined by mass-flow ratio. These losses were two or three times the theoretical shock losses. The losses up to the canopy station were negligible; losses attributed to the angle of attack of 3° were determined to be only about 2 percent of the free-stream total pressure. Therefore, to aid in explaining these losses, inlet-entrance rake profiles are shown in figure 15(a) for a flight Mach number of 2.0 and a range of diffuser-discharge Mach numbers (mass-flow ratios).

The high-energy core of the profiles is in agreement with the theoretical shock losses. The difference between the realized and theoretical losses is caused by boundary-layer accumulation or separation on the compression surface (cone) and in the region bounded by the floor and sides of the cowling and semicone (hereinafter referred to as valleys).

As the flight Mach number is reduced, the region of low-energy air at the compression surfaces and in the valleys is decreased, as indicated in figure 15(b). Inlet profiles for the cone in the aft position are shown in figure 15(c) for various flight Mach numbers. As the flight Mach number is increased, a region of low-energy air appears near the cowl lip because the cowl is not properly positioned with regard to the conical shock.

The radial and circumferential distribution of total-pressure recovery at the diffuser exit is of interest for determining the effect of these flow conditions on ram-jet combustion-chamber design or on the performance of turbojet engines. Figure 16 is a map of total-pressure contours at the diffuser exit for the $M_0 = 2.0$ cone position at a flight Mach number of 2.0. The core of high-energy air appears in the upper right-hand quadrant; low-energy air appears in the region of the duct that has undergone the greatest amount of turning and that initially had low-energy air at the inlet.

[redacted]

The flow at the diffuser exit was not separated inasmuch as diametral plots of the exit-rake profiles indicated that the measured static pressures were less than the lowest measured total pressure. Some separation of the flow was present in the subsonic diffuser forward of the exit. An example of the longitudinal and lateral distribution of flow separation 1/4 inch from the floor of the diffuser is shown in figure 17. In general, the flow (1/4 inch from surface) in the windward valley and over the tail of the afterbody was separated for the $M_0 = 2.0$ cone position. For the $M_0 = 1.5$ cone position, some flow separation was present in the region of the afterbody tail at flight Mach numbers of 1.9 and 2.0.

Redesigned inlet with sweptback splitter plate. - In addition to the straight leading-edge splitter plate previously discussed, a splitter plate with a sweptback leading edge (included angle of 96° from cone tip to cowling) was investigated. Inlet performance for the sweptback splitter plate with 0.73 (maximum) and 0.43 boundary-layer-duct mass-flow ratios at a flight Mach number of 2.0 and an angle of attack of 3° is presented in figure 18. The sweptback-splitter-plate inlet had a stable subcritical operating range of about 18 percent of the critical mass-flow ratio as compared, at equal boundary-layer-duct mass-flow ratio, with 12 percent obtained with the straight splitter plate (see fig. 13(a)); peak total-pressure recoveries were about the same for both configurations. Reference 2 predicted that a sweptback splitter plate with suction slots parallel to the plate leading edge capable of complete removal of the boundary-layer air would be advantageous compared with the straight splitter plate. The boundary-layer duct of the configuration investigated herein was not large enough to permit ducting all the boundary-layer air existing across the width of the inlet. By integrating the canopy boundary-layer profile for $h/\delta = 1.0$ ($\delta = 0.8$ in.), the percentage of air that must be spilled out the open scoop sides (based on width of cowling) was determined as:

$\left(\frac{m_d}{m_0}\right)_b$	Air spilled (percent)
0.73 (maximum)	41
.43	65

Operating the boundary-layer duct at maximum capacity reduced the main inlet pressure recovery of the sweptback-splitter-plate inlet as much as 2 percent in the subcritical region, decreased the inlet losses, and increased the internal duct losses (see fig. 18).

The increase in drag coefficient for maximum boundary-layer-duct flow was approximately constant over the range of inlet mass-flow ratios and is primarily associated with the momentum decrement or friction losses caused by the additional mass flow entering the boundary-layer ducts.

[redacted]

Performance of redesigned inlet at angle of attack. - For a flight Mach number of 2.0 and the $M_0 = 2.0$ cone position, the inlet performance for angles of attack of 0° to 12° is presented in figure 19(a) for the straight splitter plate and in figure 19(b) for the sweptback splitter plate. For both configurations the reduction in peak total-pressure ratio with angle of attack was appreciable, decreasing from 0.88 at 0° to 0.71 at 12° for the straight splitter-plate inlet and to 0.70 for the sweptback splitter-plate inlet at 12°. The noticeable difference between the inlet performance with the two splitter plates is the extension of the stable subcritical operating range for the sweptback design at angles of attack of 0°, 3°, 6°, and 9°.

Inlet performance for the $M_0 = 1.5$ cone position and the straight leading-edge splitter plate is shown in figure 20 for a flight Mach number of 1.5 for angles of attack from 0° to 12°. At a flight Mach number of 1.5, the inlet is relatively insensitive to angles of attack from 0° to 9°.

Flow approach angles measured in a single plane parallel to the canopy surface at station 68.6 are presented in table I for a range of flight Mach numbers and angles of attack. For a flight Mach number of 2.0 at the design cruise angle of attack of 3°, the flow is approaching the inlet axis at $3\frac{1}{2}^\circ$; at zero angle of attack, the flow deflection is about $\frac{1}{2}^\circ$. Thus, the pressure recovery and mass-flow characteristics of the inlet obtained at 0° (fig. 19) may be indicative of the performance that could be expected with the fuselage at an angle of attack of 3° and the inlet axis canted -3° in the direction of the local flow.

Typical inlet total-pressure-ratio profiles for each cone position at design Mach number are presented in figure 21 for various angles of attack. For a flight Mach number of 2.0, progressive deterioration of the flow profile of the windward inlet rakes is shown as the angle of attack is raised (fig. 21(a)); at an angle of attack of 12°, the windward rakes indicate separated flow except near the surface of the semicone. At a flight Mach number of 1.5, deterioration of the windward inlet rake profile is not indicated until the angle of attack is 12° (fig. 21(b)), which is the same trend observed for the variation of total-pressure recovery with angle of attack. Internal separation data showed that the lateral and longitudinal distributions in a single plane 1/4 inch from the diffuser floor was not severely affected by angle of attack, although the separation may extend higher than the plane of measurement.

Maps of total-pressure contours at the diffuser exit for angles of attack of 0°, 9°, and 12° are shown in figure 22. The high-energy

core of air is effectively rotated counterclockwise as the angle of attack is increased. A small region of separated flow is indicated for an angle of attack of 9° and an appreciably larger region for an angle of attack of 12°.

Performance of redesigned inlet at flight Mach numbers of 0.63 and 0. - For turbojet-powered aircraft the subsonic and take-off performance of supersonic inlets is of interest. Total-pressure recoveries and mass-flow ratios for the aft or $M_0 = 1.5$ cone position are presented in figure 23 for a flight Mach number of 0.63 and angles of attack from 0° to 9°. Mass-flow ratio is based on free-stream density and velocity and minimum inlet area. The diffuser-discharge Mach numbers were computed from mass flow and total pressure to satisfy one-dimensional continuity. In reference 3 a method of averaging local diffuser-discharge Mach numbers from pressure rake data was used to present the pressure recoveries at subsonic conditions for the inlet with the centerbody removed.

Pressure recovery for critical mass flow varied from 0.97 at zero angle of attack to about 0.90 at an angle of attack of 9°. The critical mass flow, at $\alpha = 0°$, was about 91 percent of the maximum theoretical mass flow calculated for choking at the minimum area, thus indicating the magnitude of the vena contracta. Evaluation of external cowling pressure distribution (uncorrected for tunnel effects) indicated a critical flight Mach number of 0.78 at an angle of attack of 3° for critical mass-flow ratio, according to the Kármán-Tsien extrapolation.

Air-flow requirements for engine B of reference 5 could be satisfied at a pressure recovery of about 0.89 at zero angle of attack at sea level, as indicated on figure 23; however, the inlet-engine matching point is in the low-pressure recovery region of constant mass flow. For turbojet engines operating at constant rotational speed the Mach number at the face of the compressor increases with increasing altitude; thus, performance at altitude would be limited for the particular engine illustrated (see fig. 23) unless the minimum inlet flow area was increased.

Inlet rake total-pressure-ratio profiles are presented in figure 24 for a flight Mach number of 0.63 and various angles of attack. Deterioration of the flow profile on the windward side of the inlet is indicated at an angle of attack of 9°.

Inlet performance at zero flight Mach number with the aft cone position is presented in figure 25. Mass-flow ratio is based on ambient pressure and minimum inlet area. Pressure recoveries greater than 0.90 were attainable only at mass-flow ratios of less than 0.47 because of

the vena-contracta effect. The size of vena contracta is illustrated by the leveling off of the mass-flow curve at ratios of about 0.71 compared with a theoretical ratio of unity. Therefore, minimum inlet area would need to be increased by some technique such as "blow-in" doors or the translating slotted cowling reported in reference 6, unless the thrust loss associated with the low-pressure recoveries could be tolerated for take-off.

SUMMARY OF RESULTS

The performance of scoop inlets was investigated over a range of supersonic Mach numbers from 1.5 to 2.0 at angles of attack from 0° to 12° as well as at subsonic Mach numbers of 0 and 0.63. The inlets were mounted in a distorted flow on the fuselage of a proposed airplane. The inlets utilized half of a conical spike as the compression surface and ram boundary-layer scoops. In order to simulate a variable-geometry inlet, the semicone was investigated in two longitudinal positions. Two types of splitter plates were used to separate the flow entering the boundary-layer duct and the main inlet. The following results were obtained:

1. A peak pressure recovery of 0.86 was attained for subcritical operation at a flight Mach number of 2.0 (local Mach number of about 1.83) and an angle of attack of 3° with complete removal of the fuselage boundary layer forward of the inlet and the semicone in the forward position. Pressure recoveries of 0.95 were obtained at a flight Mach number of 1.5 (local Mach number of 1.39). The inlet captured practically all the local stream tube at a flight Mach number of 2.0 and a pressure recovery of 0.83, but spilled about 12 percent of the local stream tube at a flight Mach number of 1.5.

2. Translating the semicone to the aft position decreased the mass-flow spillage to 7 percent at a flight Mach number of 1.5 with no significant change in pressure recovery. At flight Mach numbers of 1.9 and 2.0, the inlet operating range with the aft cone position was severely limited by pulsing, and pressure recovery was substantially reduced.

3. At a flight Mach number of 2.0, peak total-pressure recovery varied from 0.88 to 0.70 over the angle-of-attack range of 0° to 12°. At a flight Mach number of 1.5, inlet performance was relatively insensitive to variations of angle of attack from 0° to 9°.

4. With a straight leading-edge splitter plate, the stable subcritical range was 12 percent of the critical mass flow at a flight Mach number of 2.0 and an angle of attack of 3° with cone in a forward

position. Sweeping back the splitter-plate leading edge increased the stable subcritical range to 18 percent of the critical mass flow; peak pressure recovery was not changed. The sweptback design also had a larger stable subcritical range at angles of attack of 0°, 6°, and 9°.

5. At a flight Mach number of 0.63 with the aft cone position, a pressure recovery of 0.97 was attained for critical inlet flow. The critical mass flow was only 91 percent of that theoretically possible. Tests at zero Mach number indicated the existence of a large vena-contracta effect at the inlet which limited pressure recoveries greater than 0.90 to mass-flow ratios less than 0.47; thus, take-off performance may be restricted unless some sort of auxiliary inlet is used.

Lewis Flight Propulsion Laboratory
National Advisory Committee for Aeronautics
Cleveland, Ohio

REFERENCES

1. Goelzer, H. Fred, and Cortright, Edgar M., Jr.: Investigation at Mach Number 1.88 of Half of a Conical-Spike Diffuser Mounted as a Side Inlet with Boundary-Layer Control. NACA RM E51G06, 1951.

2. Wittliff, Charles E., and Byrne, Robert W.: Preliminary Investigation of Supersonic Scoop Inlet Derived from a Conical-Spike Nose Inlet. NACA RM L51G11, 1951.

3. Weinstein, M. I.: Performance of Supersonic Scoop Inlets. NACA RM E52A22, 1952.

4. Valerino, Alfred S.: Performance Characteristics at Mach Numbers to 2.0 of Various Types of Side Inlets Mounted on Fuselage of Proposed Supersonic Airplane. I - Two-Dimensional Compression-Ramp Inlets with Semicircular Cowls. NACA RM E52E02, 1952.

5. Schueller, Carl F., and Esenwein, Fred T.: Analytical and Experimental Investigation of Inlet-Engine Matching for Turbojet-Powered Aircraft at Mach Numbers up to 2.0. NACA RM E51K20, 1952.

6. Cortright, Edgar M., Jr.: Preliminary Investigation of a Translating Cowl Technique for Improving Take-Off Performance of a Sharp-Lip Supersonic Diffuser. NACA RM E51I24, 1951.

TABLE I - INLET FLOW APPROACH ANGLE β AND MACH NUMBER M_c DETERMINED FROM STARBOARD CANOPY WEDGE BAR INSTRUMENTATION

α (deg)	M_0, 2.0			M_0, 1.9			M_0, 1.7		
	M_c	β_r	β_l	M_c	β_r	β_l	M_c	β_r	β_l
0	1.80	0°31'	0°30'	1.72	0°18'	0°16'	1.53	-0°38'	0°29'
1	1.81	1°28'	1°13'	1.74	1°22'	1°10'	1.54	0°43'	1°40'
2	1.82	2°40'	2°17'	1.74	2°40'	2°15'	1.54	2°27'	3°14'
3	1.82	3°46'	3°21'	1.74	3°41'	3°11'	1.54	4°00'	4°21'
4	1.82	4°45'	4°14'	1.74	-----	4°17'	1.53	-----	-----
5	1.82	5°30'	-----	1.73	-----	-----	1.51	-----	-----
6	1.82	6°20'	-----	1.73	-----	-----	----	-----	-----

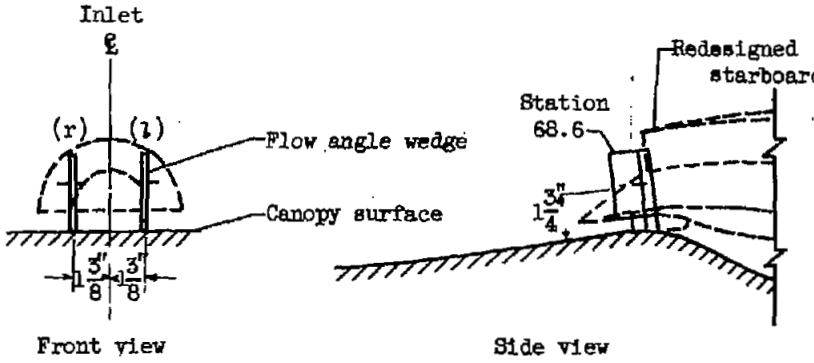

Schematic diagram showing flow angle wedges mounted on starboard canopy surface

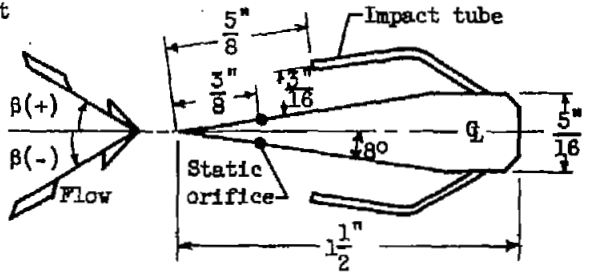

Enlarged top view of wedge bar

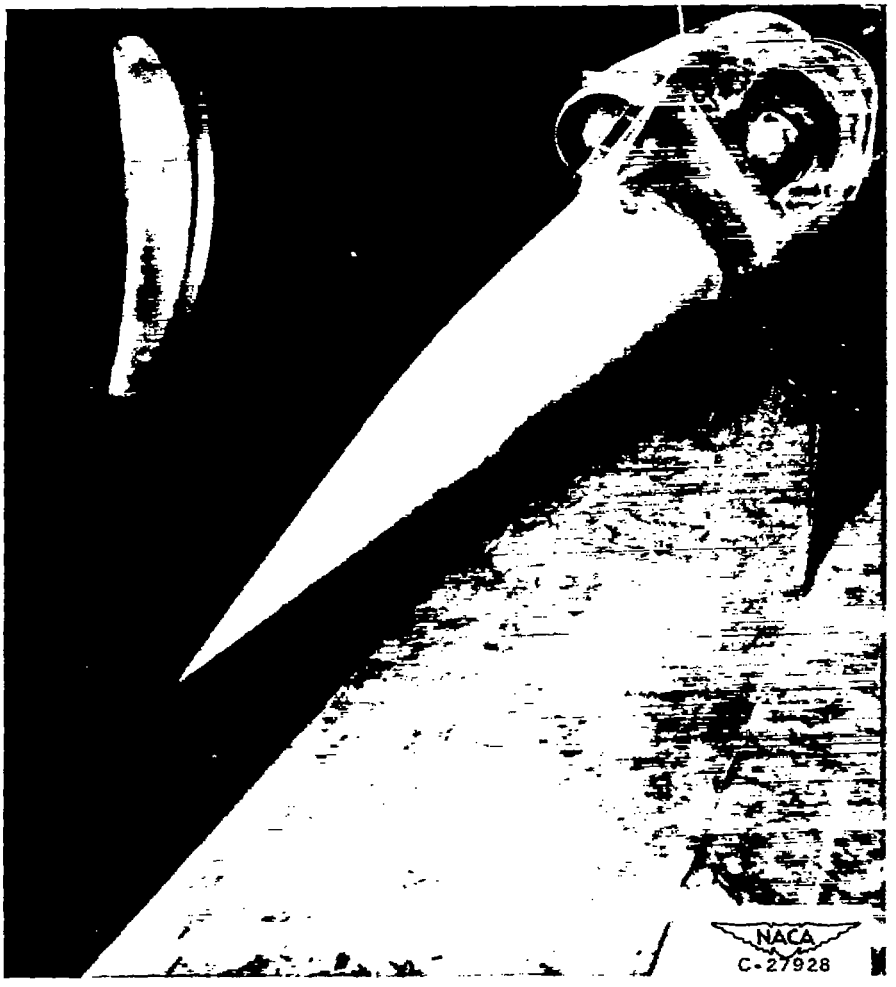

Figure 1. Photograph of model with twin semicone inlets.

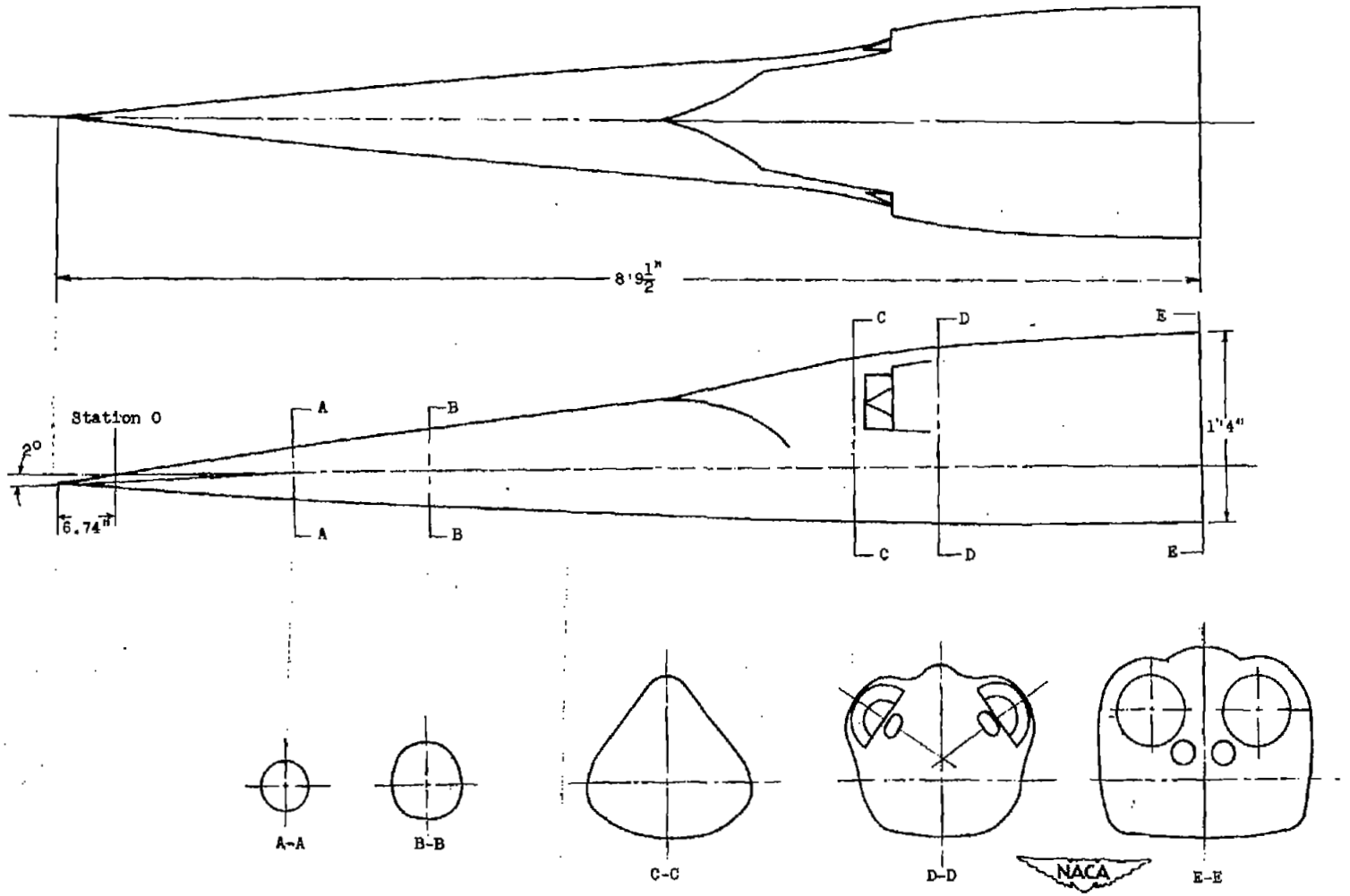

Figure 2. - Schematic diagram of model with representative cross sections.

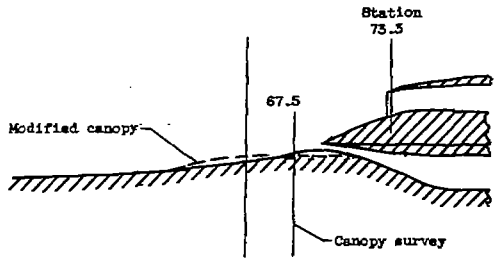

(a) First inlet.

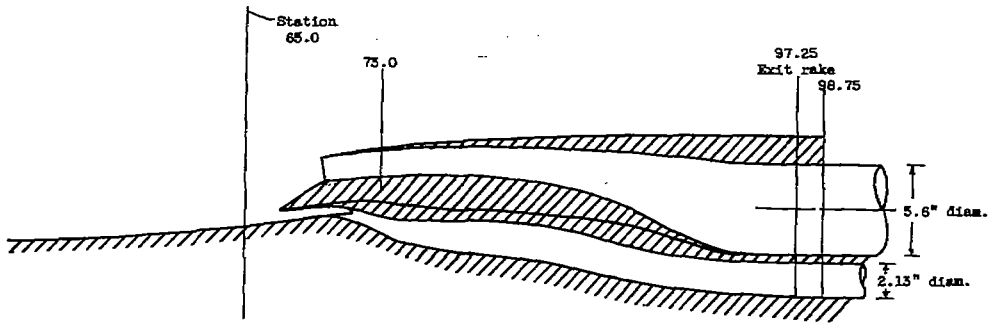

(b) Redesigned inlet.

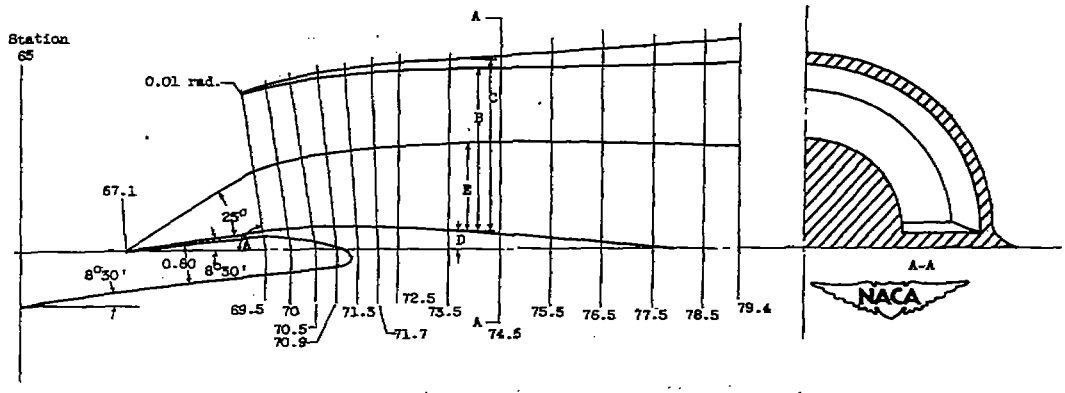

Fuselage station	A	Radius B	Radius C	D	Cone position M_0, 2.0 Radius E	Cone position M_0, 1.5 Radius E
69.5	81°50'	2.877	2.907	0.395	1.250	0.849
70	81°50'	2.935	2.990	.465	1.360	1.090
70.5	81°50'	3.020	3.085	.510	1.440	1.300
70.9	83°35'	3.070	3.180	.515	1.500	1.420
71.3	85°30'	3.120	3.260	.520	1.560	1.510
71.7	87°40'	3.170	3.320	.500	1.615	1.600
72.5	90°	3.250	3.395	.480	1.680	1.670
73.5	90°	3.350	3.530	.410	1.800	1.800
74.5	90°	3.450	3.690	.320	1.915	1.915
75.5	90°	3.560	3.860	.220	2.000	2.000
76.5	90°	3.660	4.010	.150	2.070	2.070
77.5	90°	3.760	4.150	.060	2.120	2.120
78.5	90°	3.810	4.275	.025	2.120	2.120
79.4	90°	3.855	4.327	.000	2.110	2.110

(c) Dimensions of redesigned inlet

Figure 3. - Schematic drawings of the various inlets. (Sections are normal to fuselage.) All dimensions are in inches.)

[redacted]

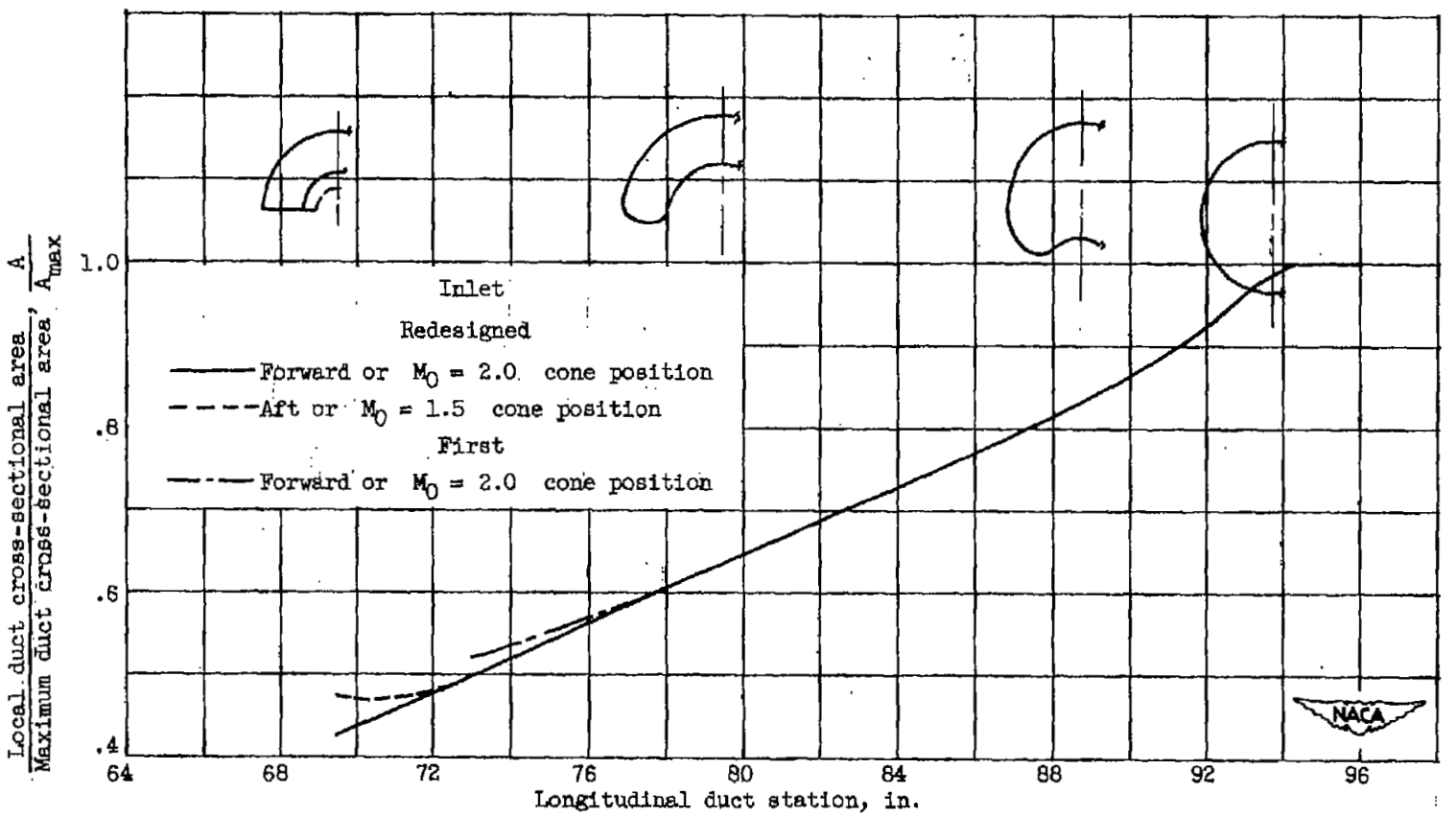

Figure 4. - Variation of local to maximum inlet area ratio with longitudinal duct station for configurations investigated. M_0, flight Mach number.

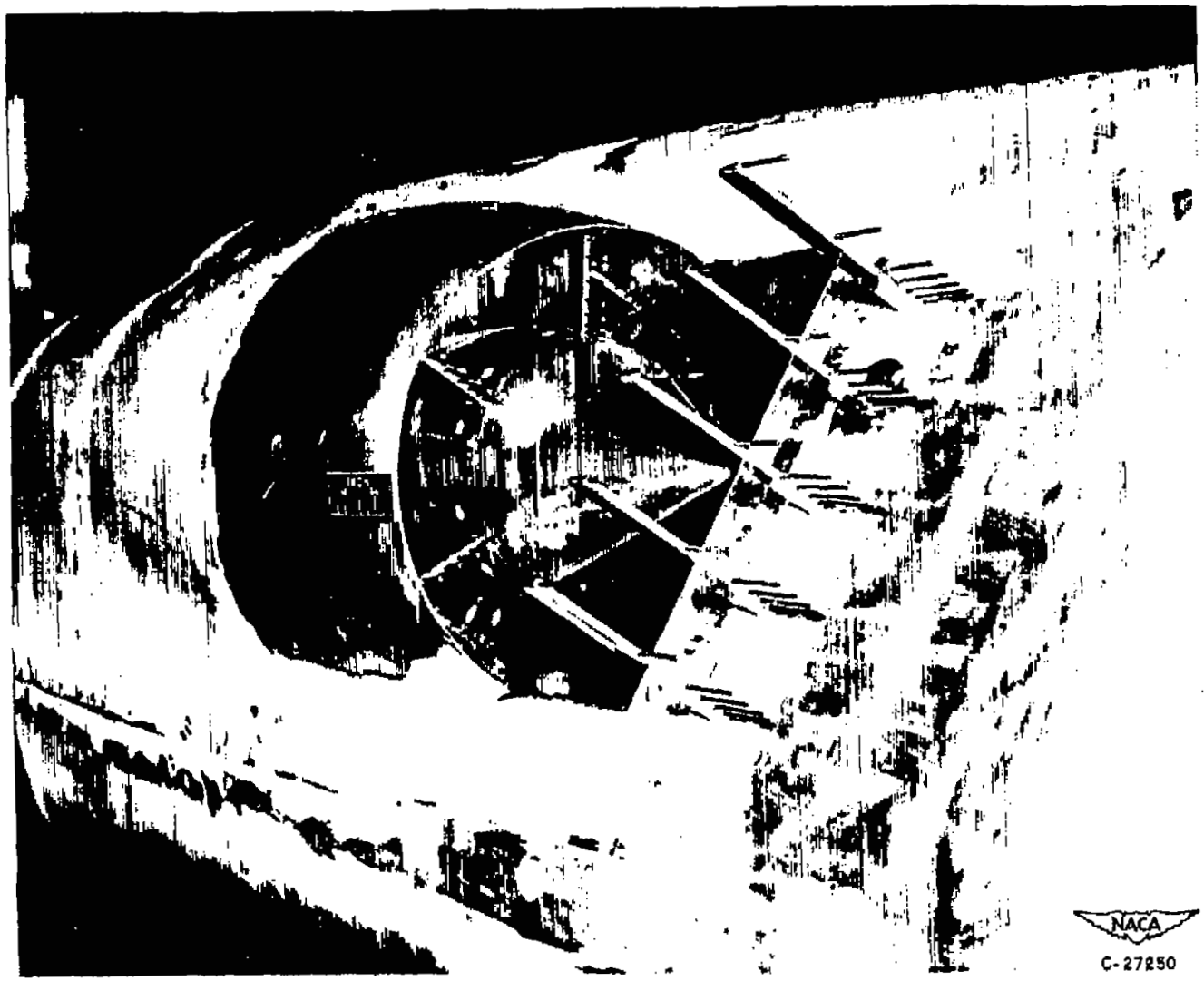

Figure 5. - Photograph of internal and removable canopy instrumentation.

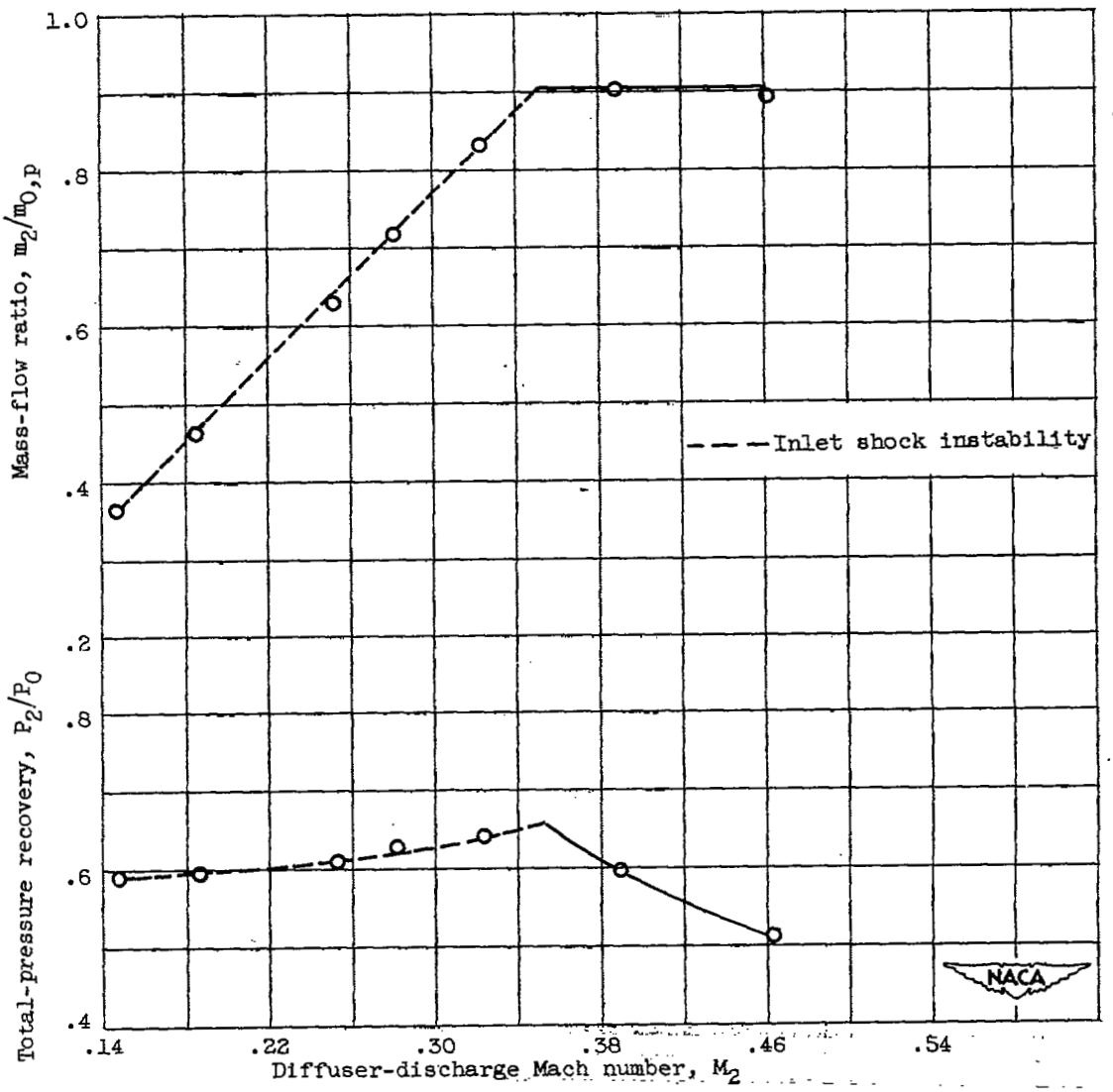

Figure 6. - Variation of inlet performance with diffuser-discharge Mach number. First inlet. Flight Mach number, 2.0; angle of attack, 3°; $h/\delta = 0.55$; $\left(\frac{m_d}{m_0}\right)_b$, 0.30; $\left(\frac{m_s}{m_c}\right)_b$, 0.38.

[redacted]

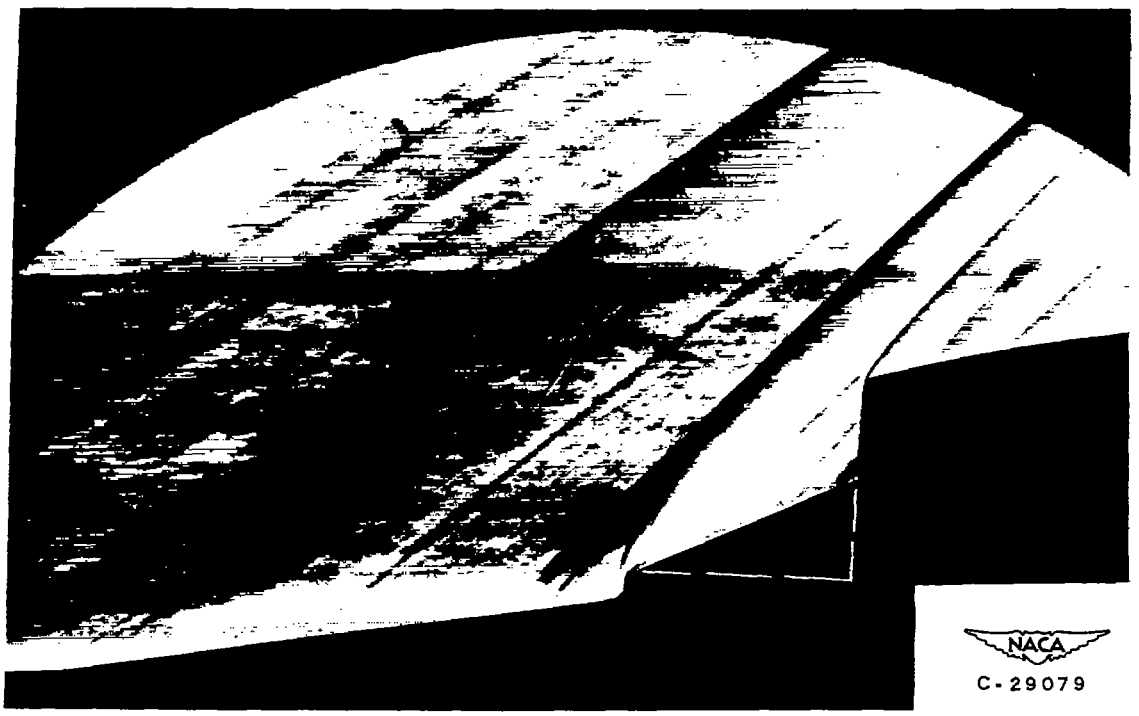

Figure 7. - Schlieren photograph of first inlet at flight Mach number of 2.0 and angle of attack of 3°. Diffuser-discharge Mach number, 0.325.

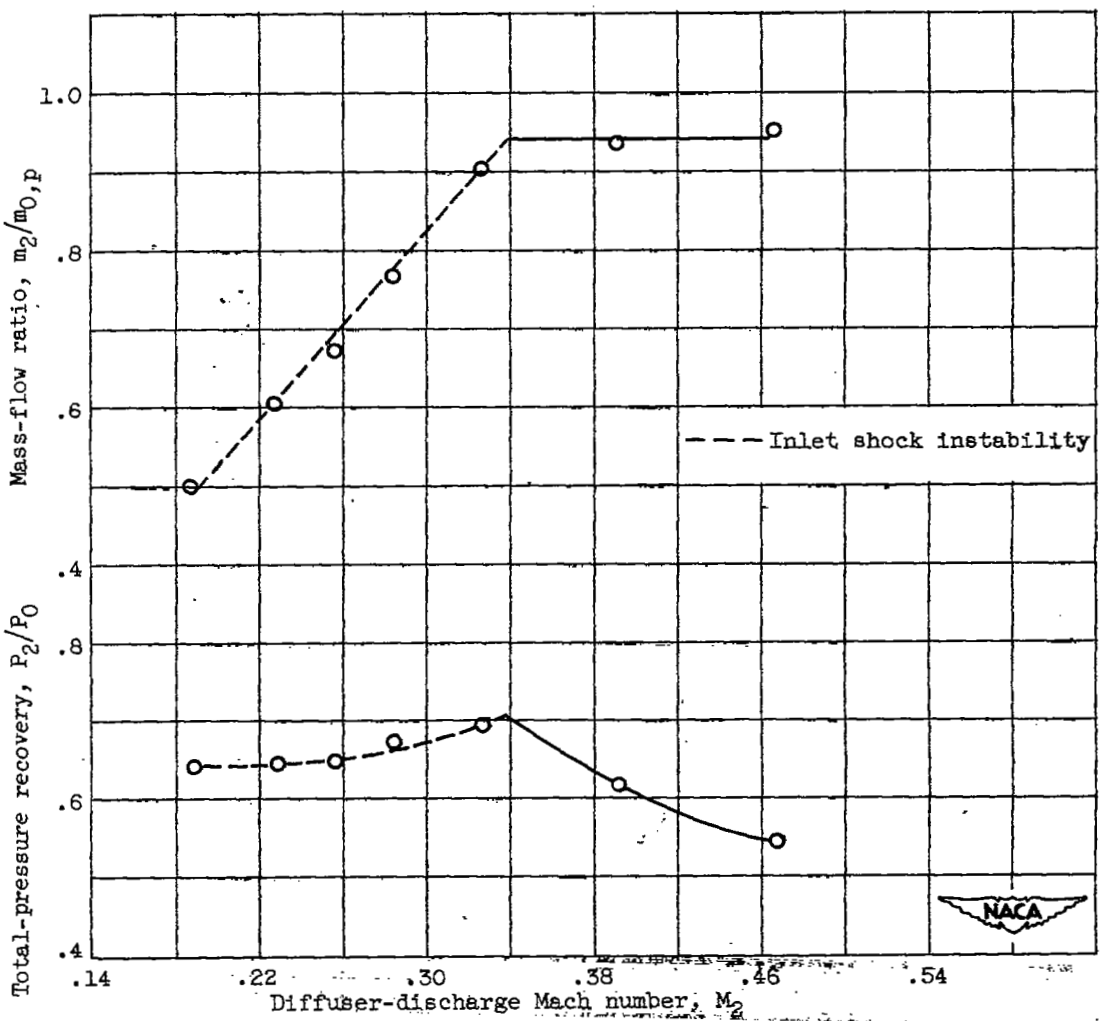

(a) $h/\delta = 0.55; \left(\frac{m_d}{m_0}\right)_b$, 0.37; $\left(\frac{m_s}{m_c}\right)_b$, 1.00.

Figure 8. - Variation of inlet performance with diffuser-discharge Mach number. First inlet, scoop sides eliminated. Flight Mach number, 2.0; angle of attack, 3°.

[redacted]

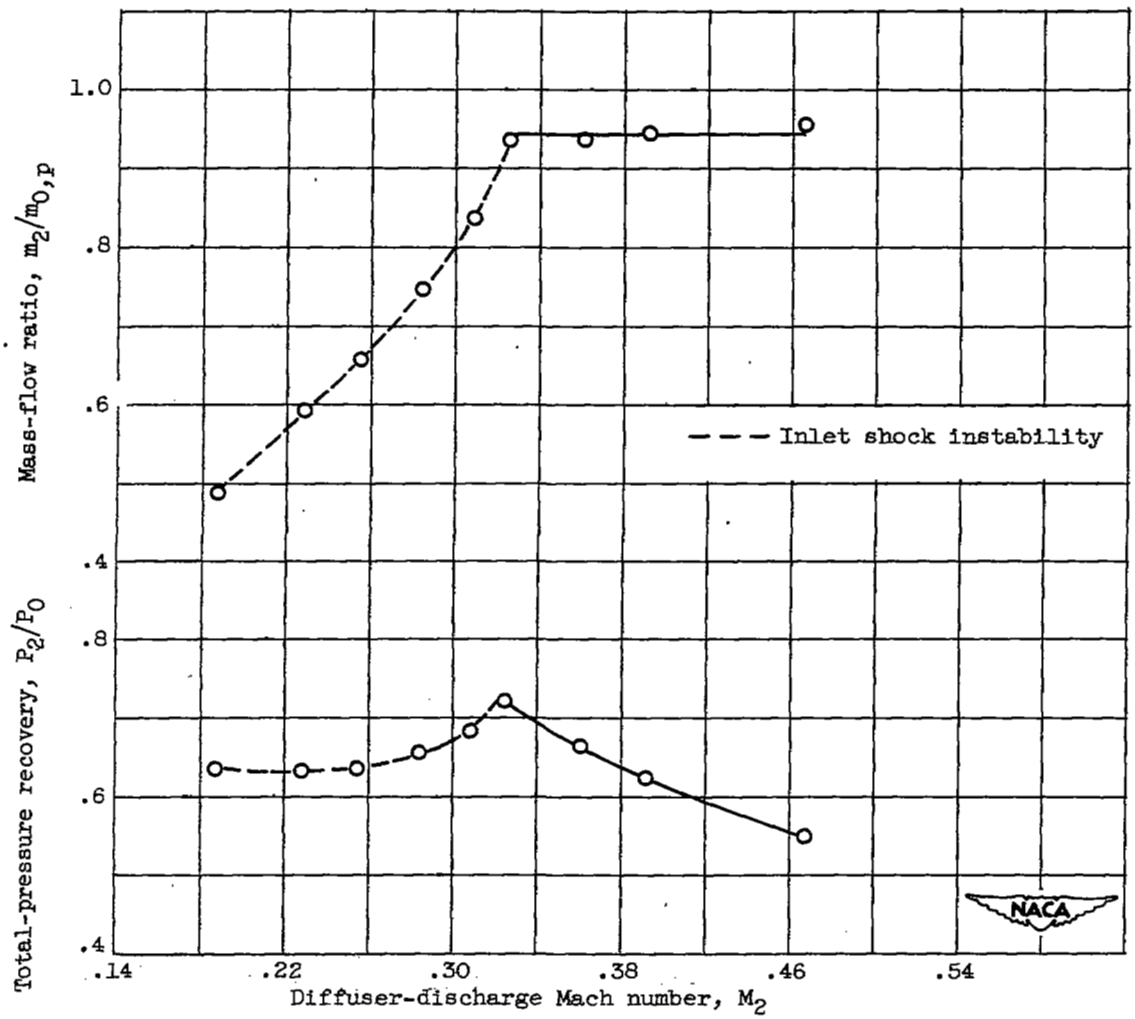

(b) Modified canopy. $0.55 < h/\delta < 1.00$; $\left(\frac{m_d}{m_0}\right)_b$, 0.53 - 0.61; $\left(\frac{m_s}{m_c}\right)_b$, < 1.00.

Figure 8. - Concluded. Variation of inlet performance with diffuser-discharge Mach number. First inlet, scoop sides eliminated. Flight Mach number, 2.0; angle of attack, 3°.

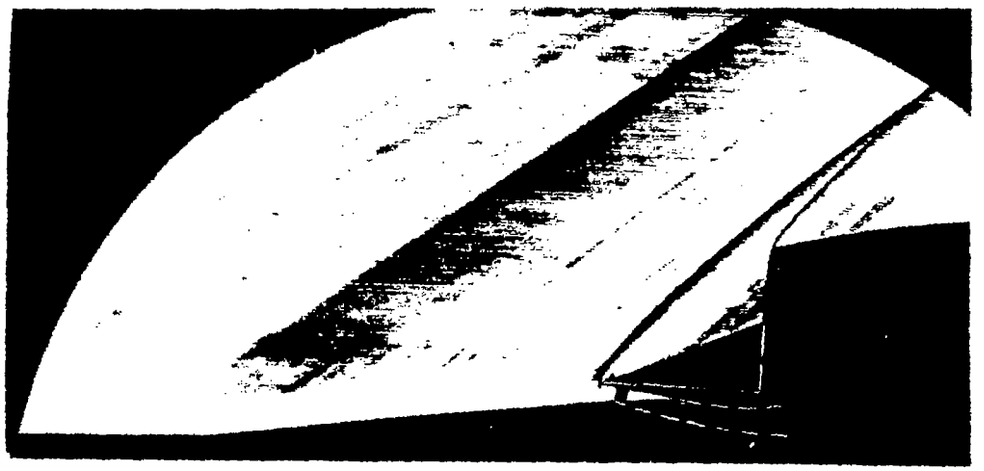

(a) First inlet, scoop sides eliminated.

NACA
C-29270

(b) First inlet, scoop sides eliminated and canopy modified.

Figure 9. - Schlieren photographs comparing modifications of the first inlet at flight Mach number of 2.0 and angle of attack of 3°. Diffuser-discharge Mach number, 0.325.

[redacted]

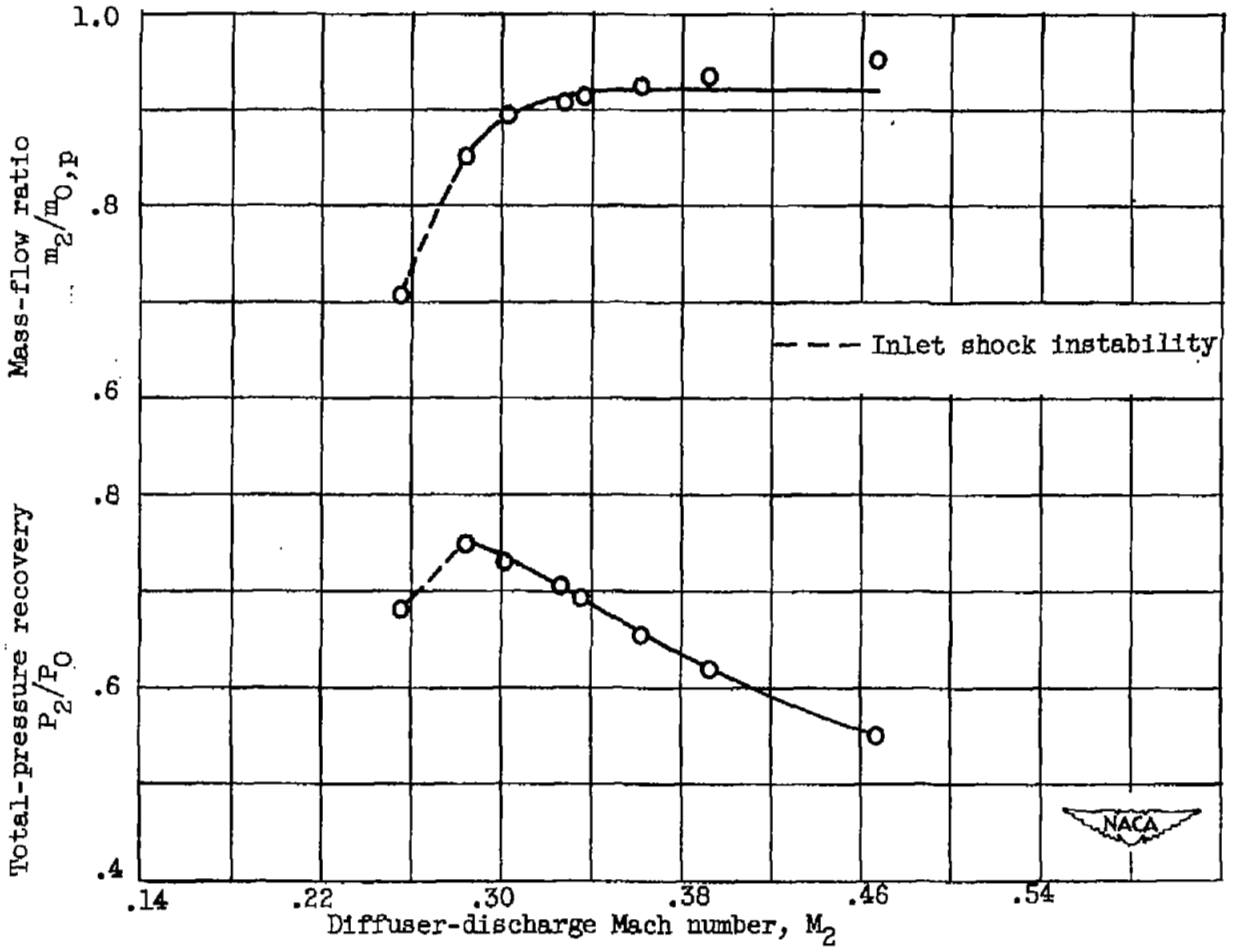

Figure 10. - Variation of inlet performance with diffuser-discharge Mach number. First inlet, scoop sides eliminated, modified canopy, and slotted cowling. Flight Mach number, 2.0; angle of attack, 3°; $0.55 < h/\delta < 1.00$; $\left(\frac{m_d}{m_0}\right)_b$, 0.56 - 0.61; $\left(\frac{m_s}{m_c}\right)_b$, < 1.00.

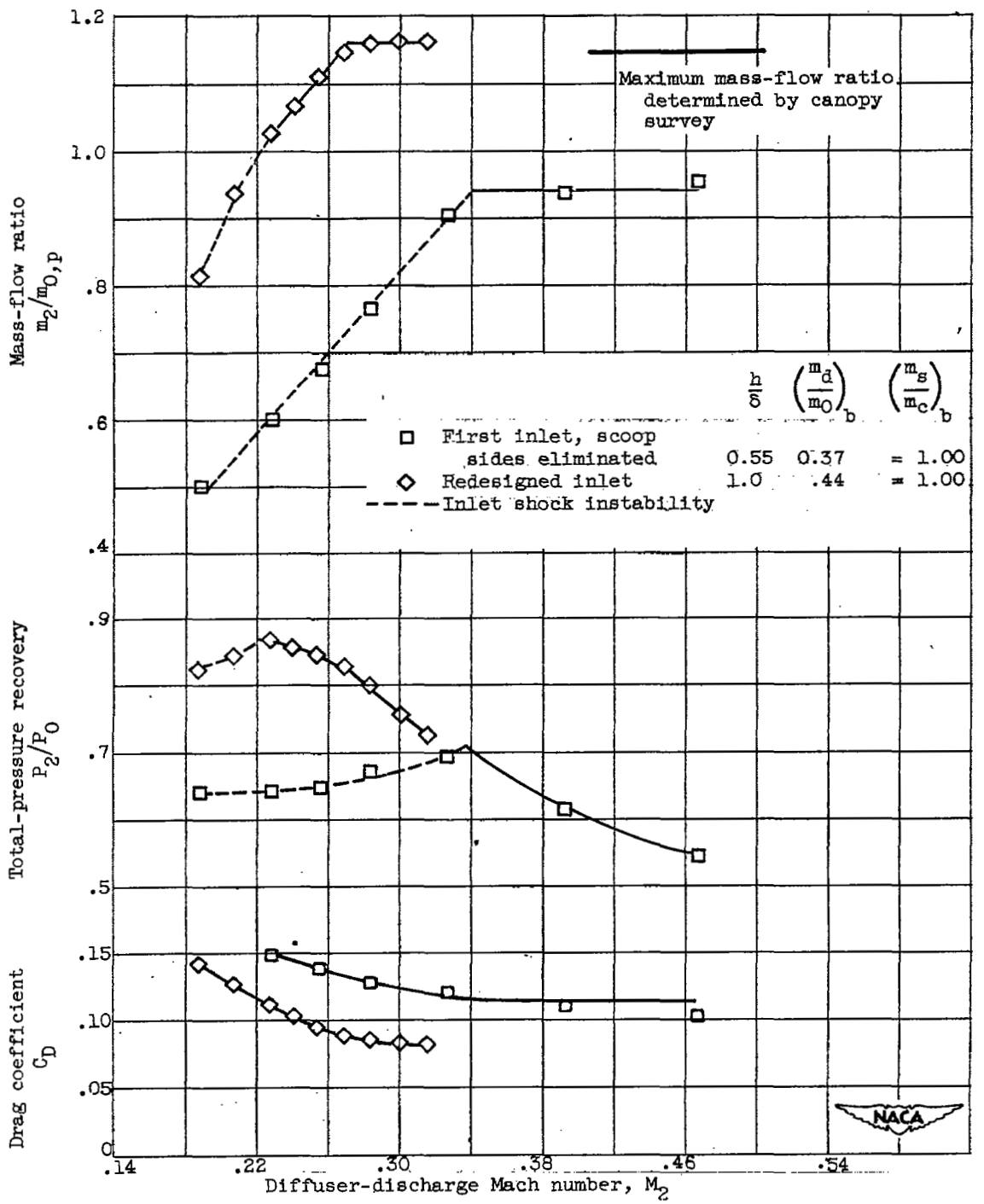

Figure 11. - Comparison of inlet performance of first inlet with scoop sides eliminated and redesigned inlet. Flight Mach number, 2.0; angle of attack, 3°.

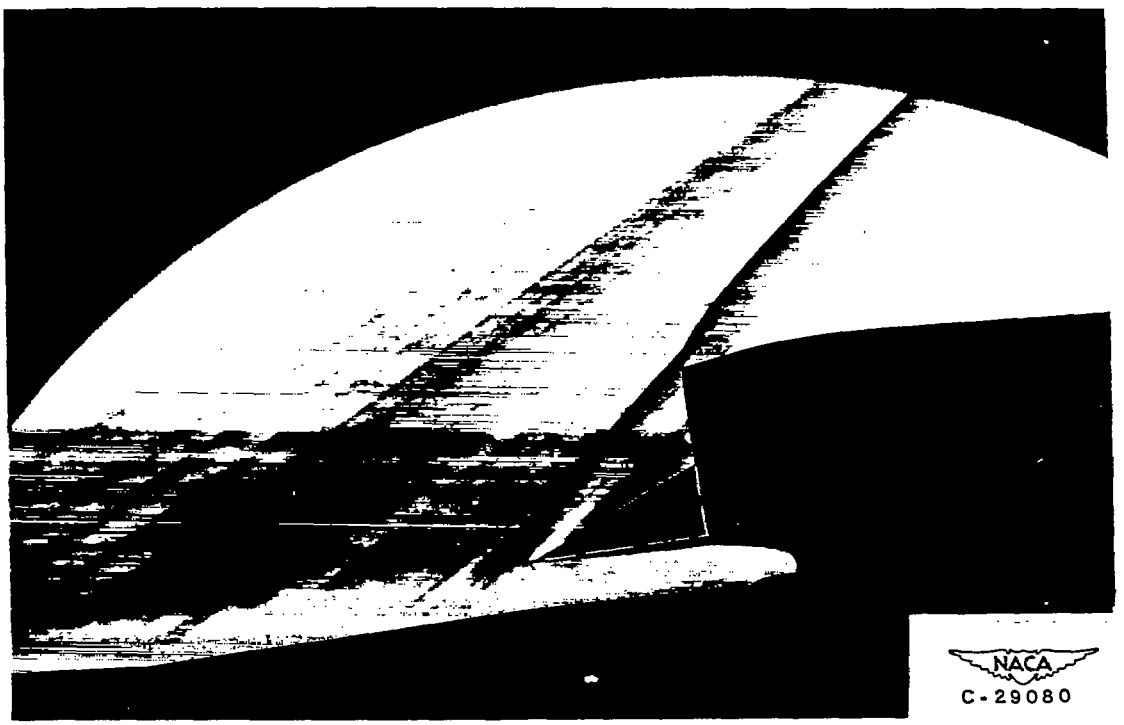

Figure 12. - Schlieren photograph of redesigned inlet at flight Mach number of 2.0 and angle of attack of 3°. Diffuser-discharge Mach number, 0.283.

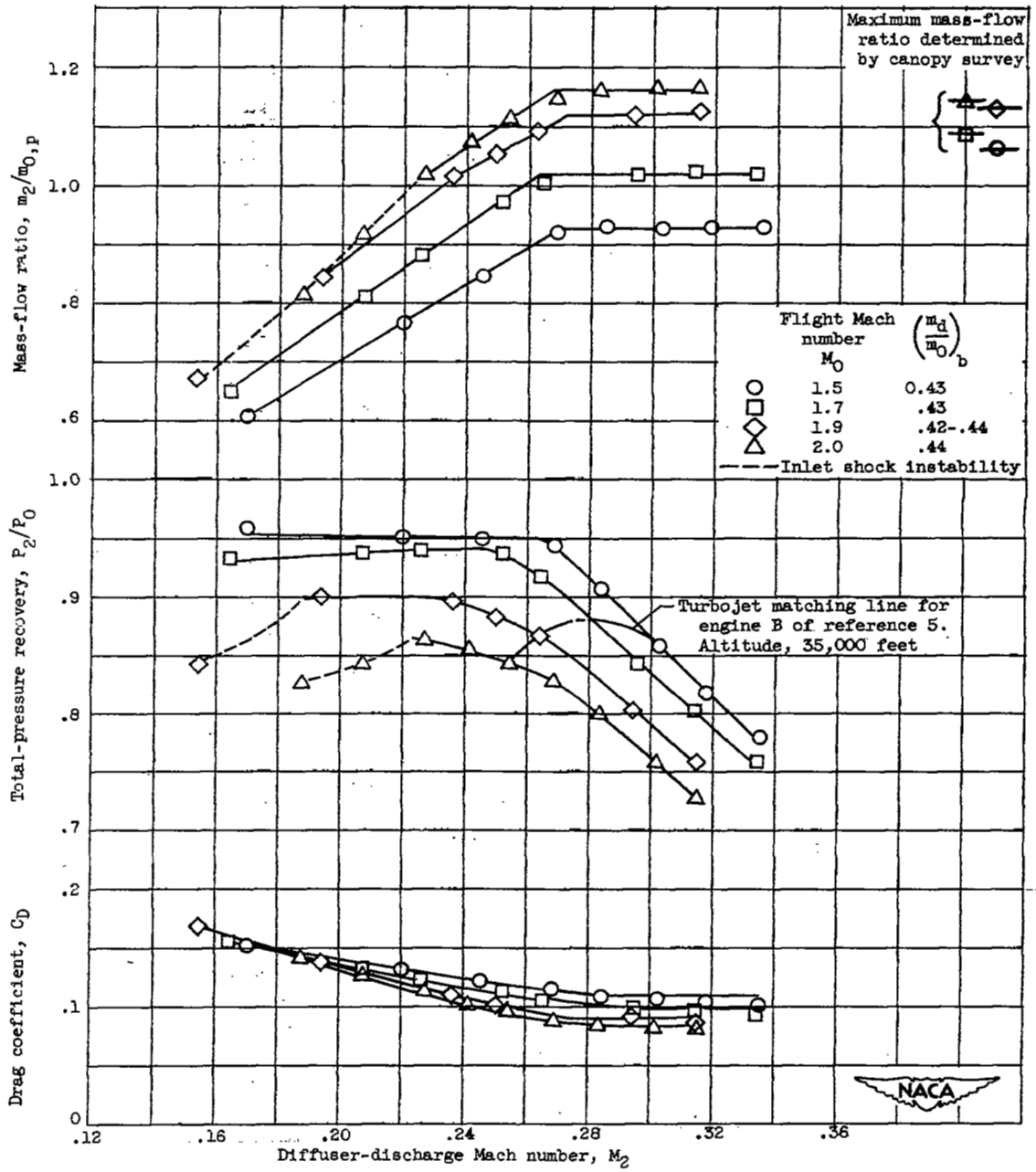

(a) Forward or flight Mach number = 2.0 cone position.

Figure 13. - Variation of inlet performance with diffuser-discharge Mach number at various flight Mach numbers for redesigned inlet. Angle of attack, 3°.

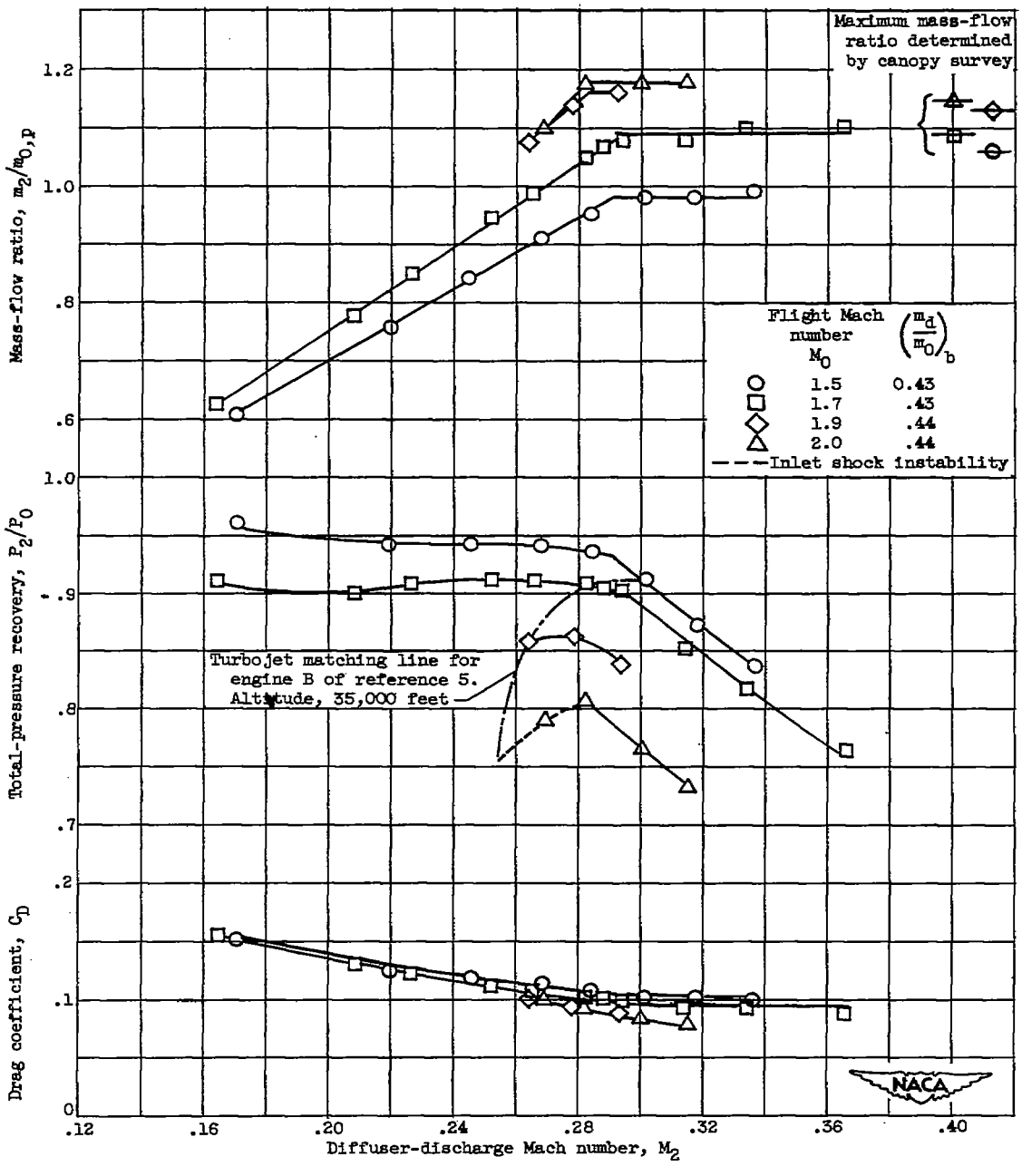

(b) Aft or flight Mach number = 1.5 cone position.

Figure 13. - Concluded. Variation of inlet performance with diffuser-discharge Mach number at various flight Mach numbers for redesigned inlet. Angle of attack, 3°.

[redacted]

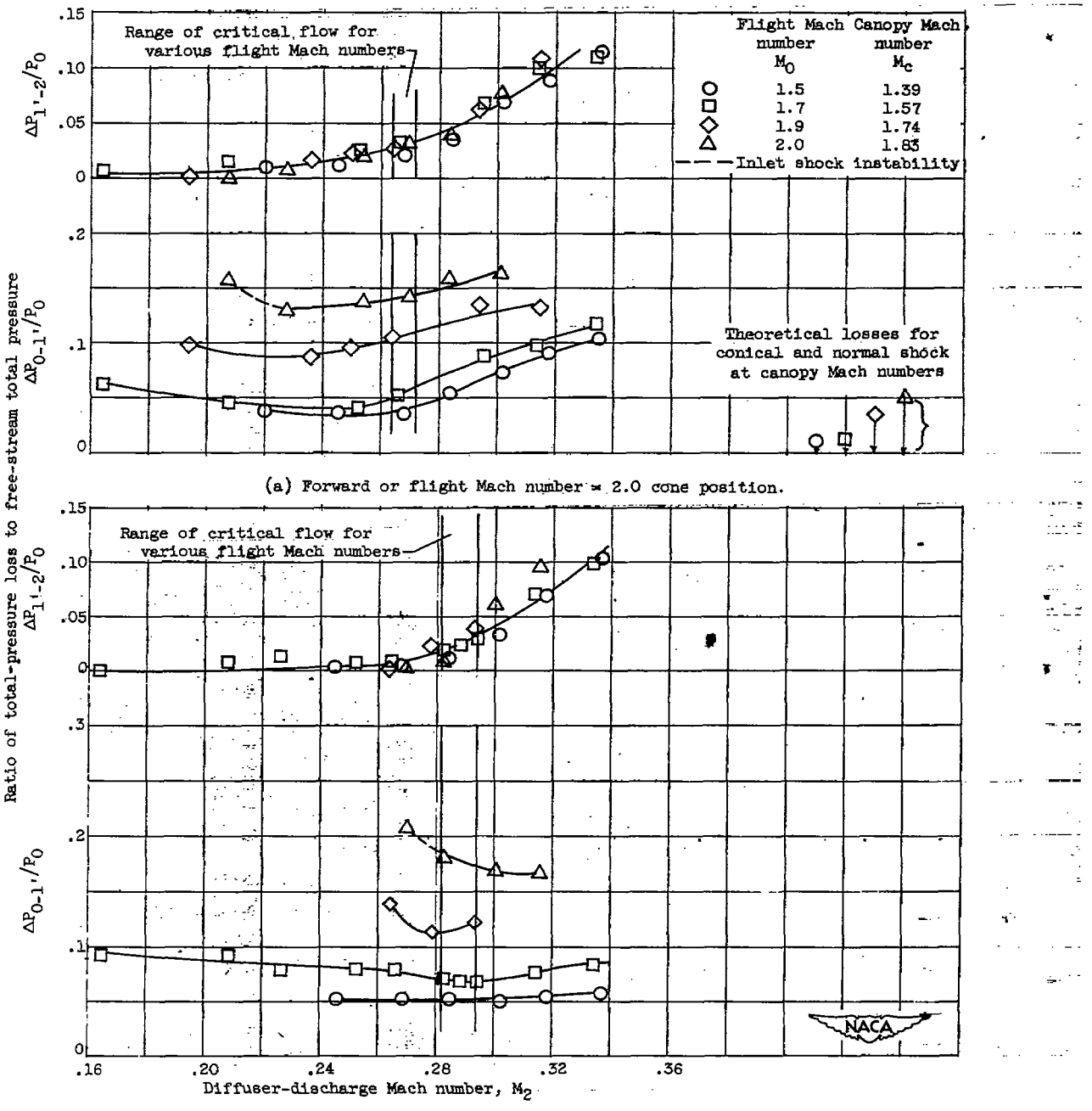

(a) Forward or flight Mach number = 2.0 cone position.

(b) Aft or flight-Mach number = 1.5 cone position.

Figure 14. - Variation of total-pressure losses with diffuser-discharge Mach number for redesigned inlet at various flight Mach numbers. Angle of attack, 3°.

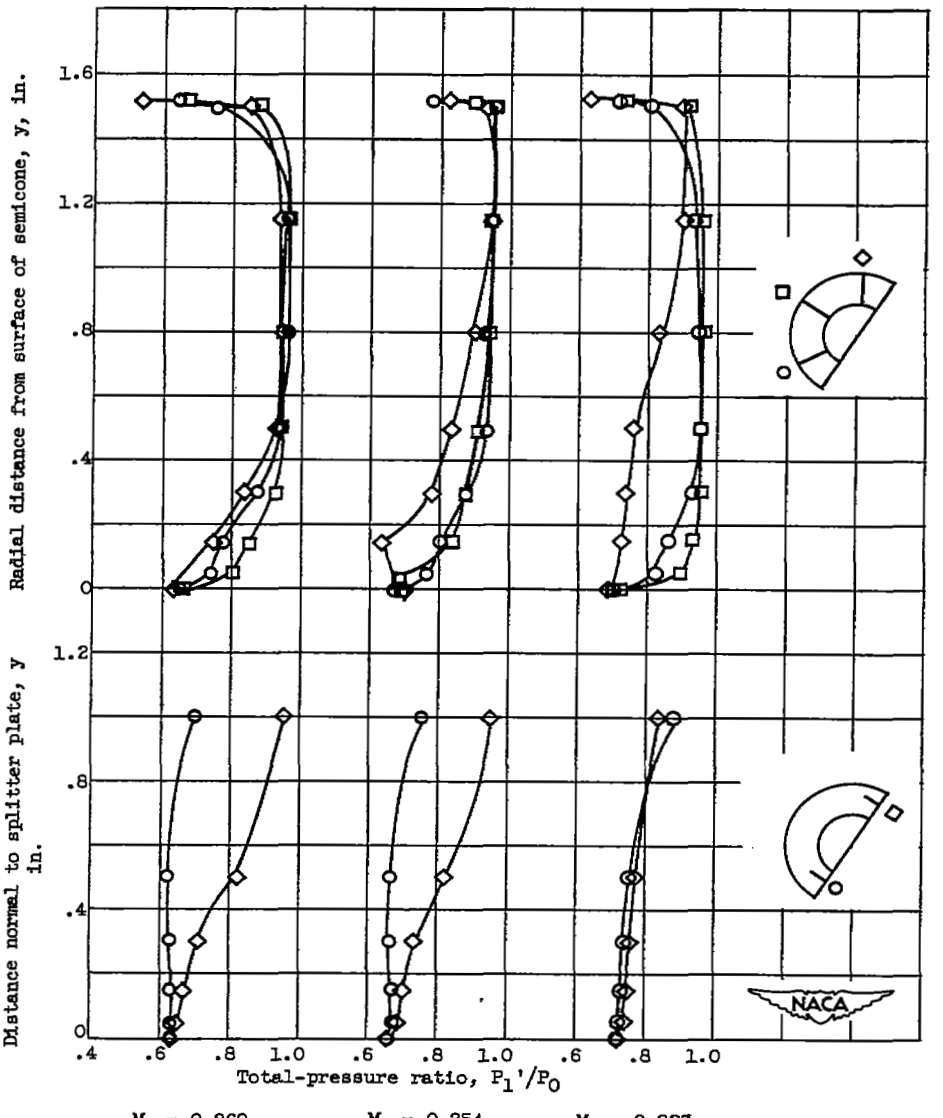

M_2 = 0.269 M_2 = 0.254 M_2 = 0.227

(a) Forward cone position. Flight Mach number, 2.0.

Figure 15. - Starboard inlet total-pressure ratio rake profiles. Angle of attack, 3°. M_2, diffuser-discharge Mach number.

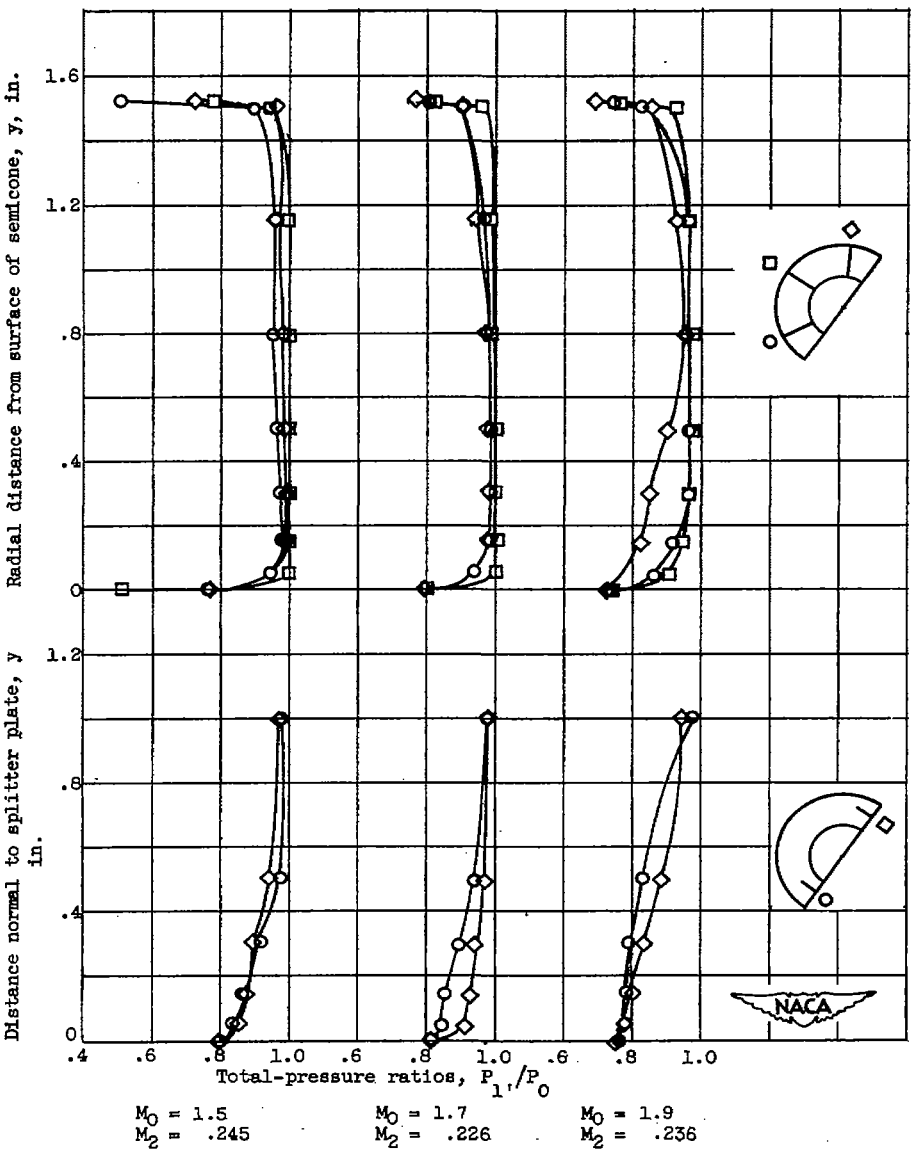

M_0 = 1.5 M_2 = .245 | M_0 = 1.7 M_2 = .226 | M_0 = 1.9 M_2 = .236

(b) Forward cone position. Various flight Mach numbers M_0.

Figure 15. - Continued. Starboard inlet total-pressure ratio rake profiles. Angle of attack, 3°. M_2, diffuser-discharge Mach number.

[redacted]

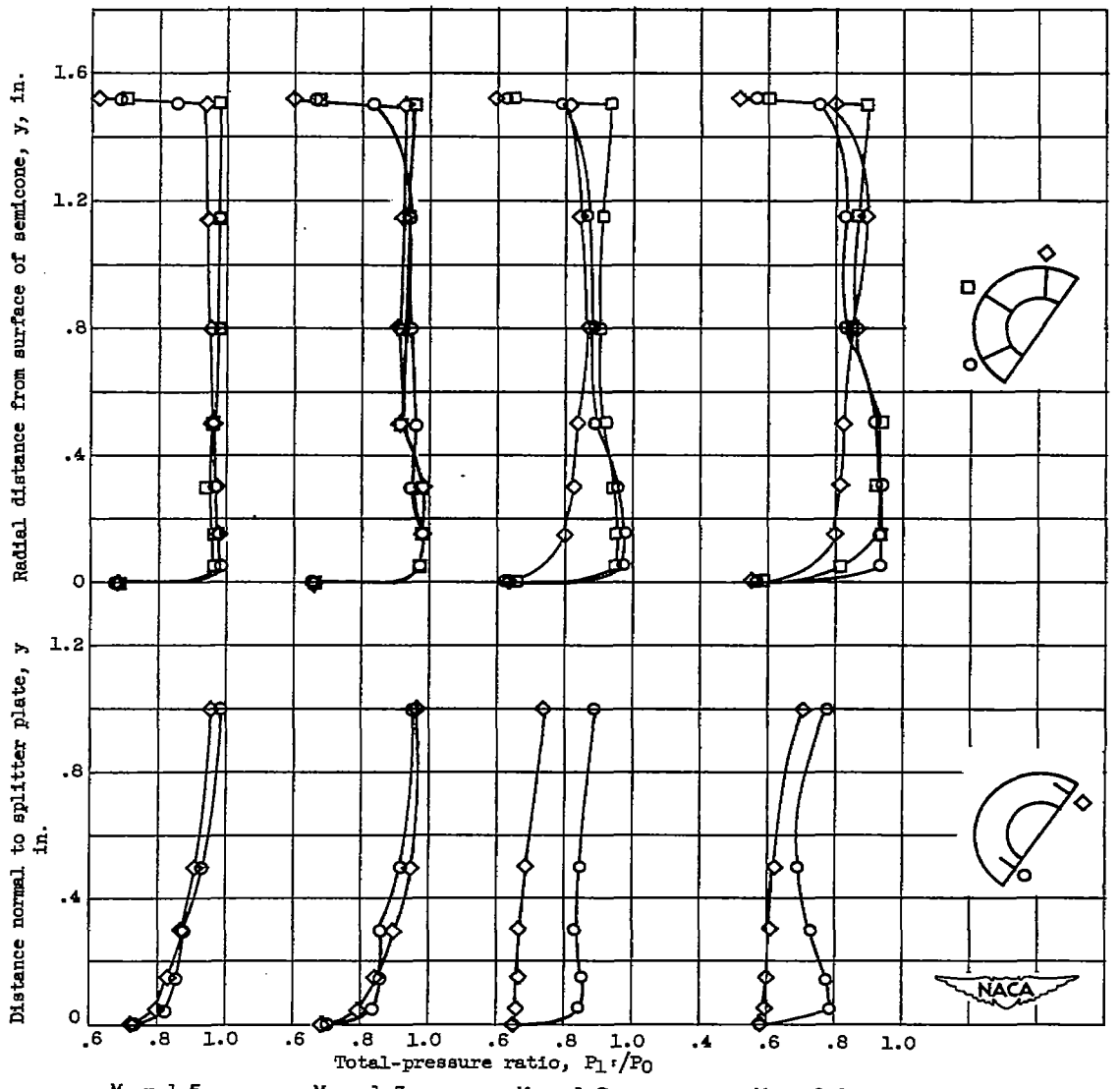

M_0 = 1.5	M_0 = 1.7	M_0 = 1.9	M_0 = 2.0
M_2 = .284	M_2 = .283	M_2 = .264	M_2 = .283

(c) Aft cone position. Various flight Mach numbers M_0.

Figure 15. - Concluded. Starboard inlet total-pressure ratio rake profiles. Angle of attack, 3°. M_2, diffuser-discharge Mach number.

[redacted]

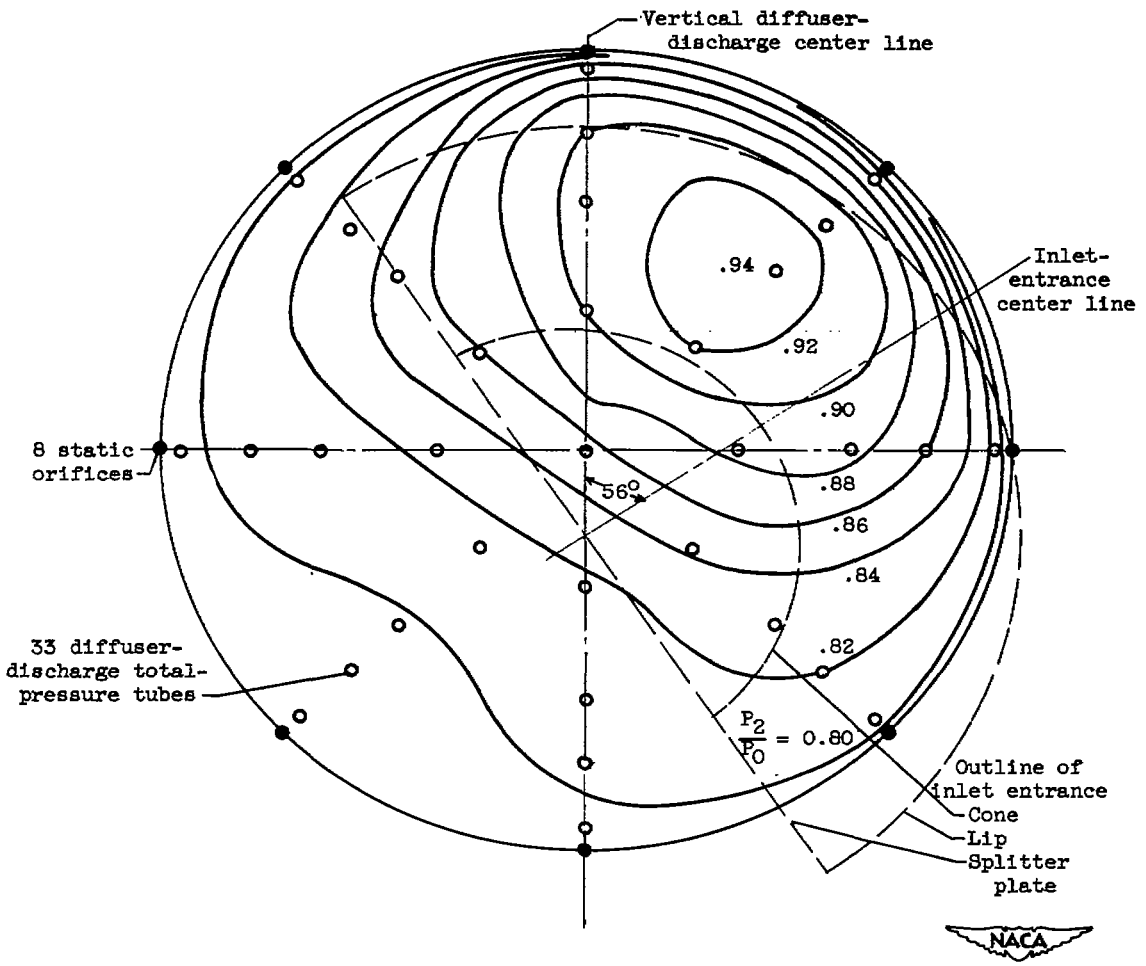

Figure 16. - Diffuser-discharge local total-pressure contours for redesigned inlet with straight splitter plate. View in plane normal to angle-of-attack axis looking aft. Flight Mach number, 2.0; diffuser-discharge Mach number, 0.254; angle of attack, 3°; pressure recovery, 0.842. Forward cone position.

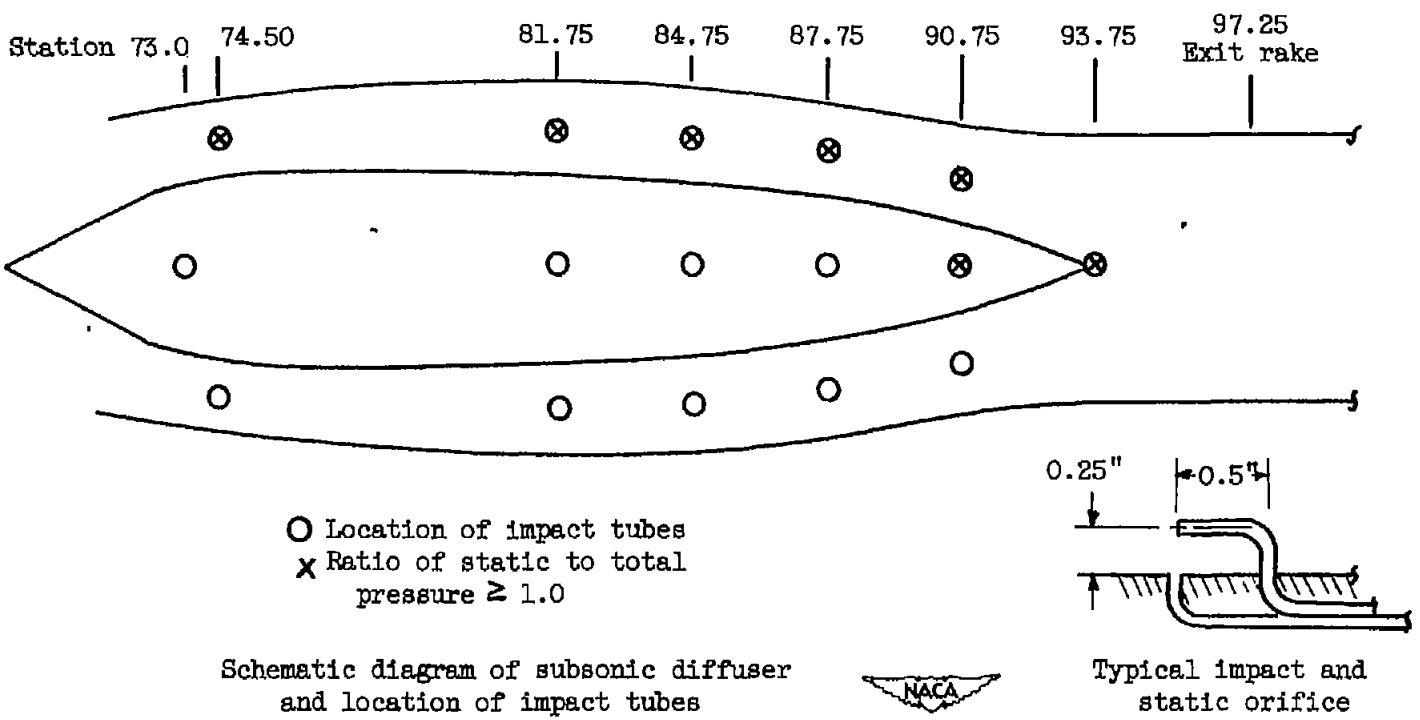

Figure 17. - Distribution of separated flow in starboard subsonic diffuser. Forward cone position. Flight Mach number, 2.0; angle of attack, 3°; diffuser-discharge Mach number, 0.269.

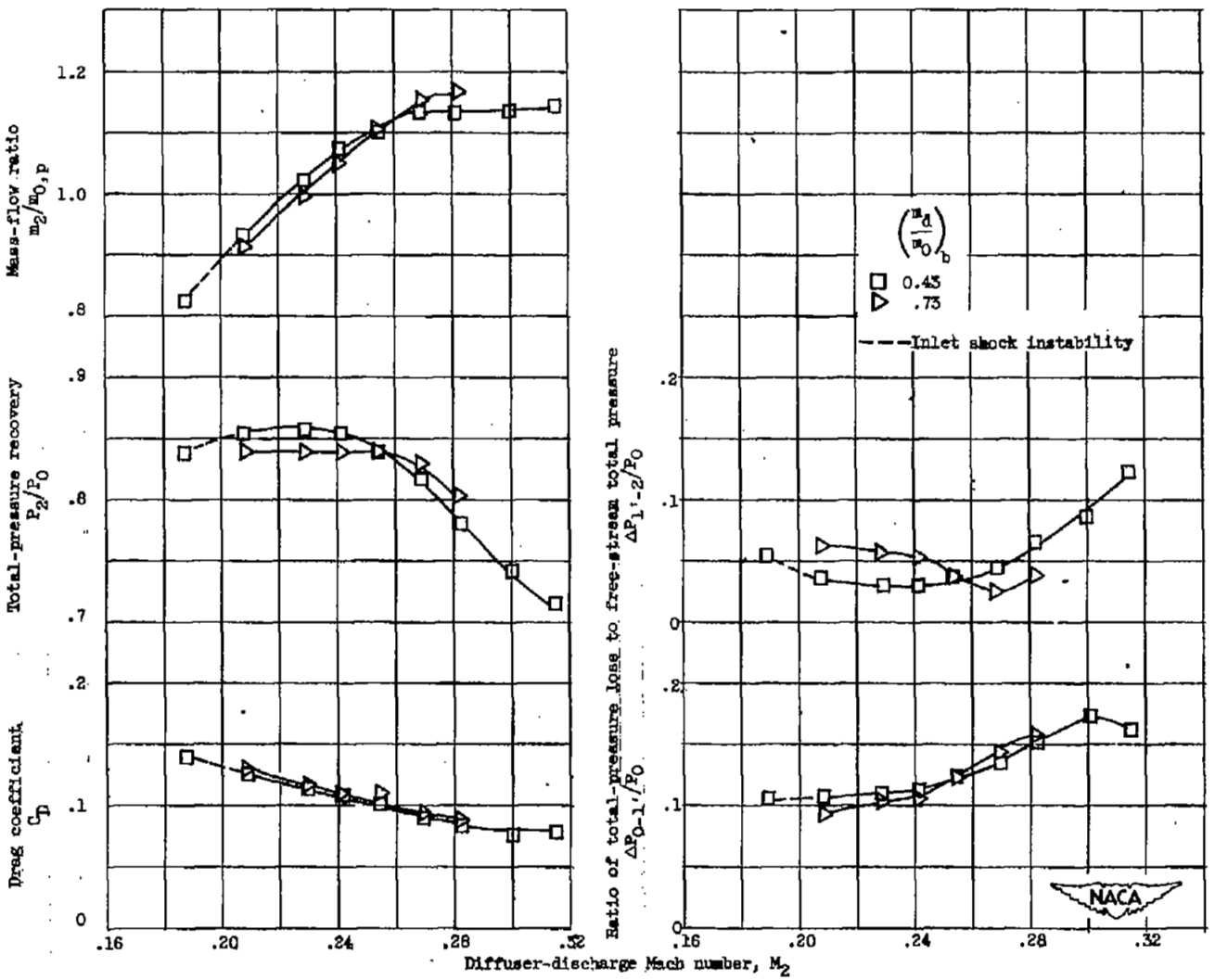

Figure 18. - Variation of inlet performance with diffuser-discharge Mach number and boundary-layer-duct mass-flow ratio for redesigned inlet with sweptback splitter plate at flight Mach number of 2.0 and angle of attack of 3°. Forward cone position.

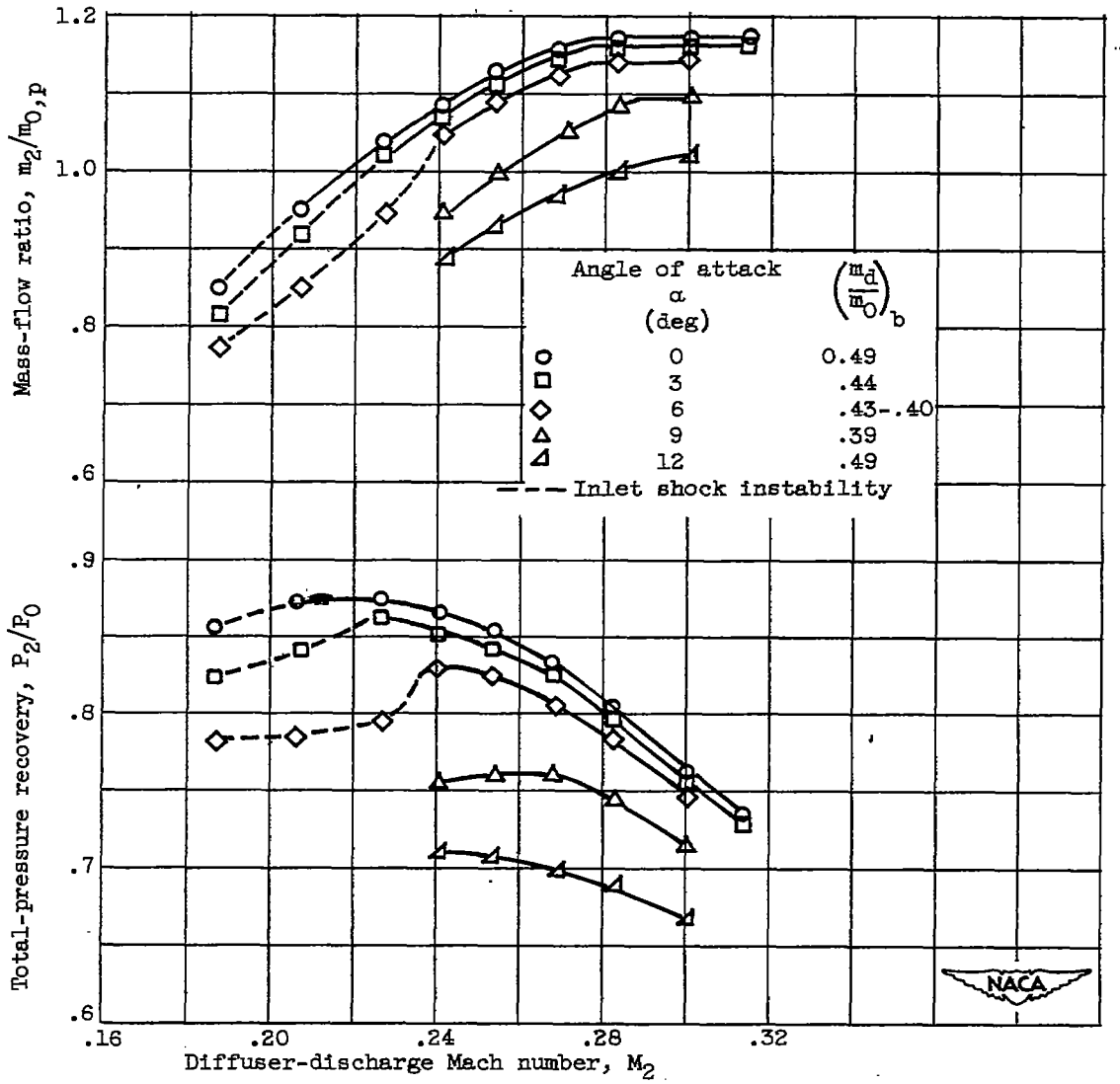

(a) Splitter plate with straight leading edge.

Figure 19. - Variation of inlet performance with diffuser-discharge Mach number at various angles of attack for redesigned inlet at flight Mach number of 2.0. Forward or flight Mach number = 2.0 cone position.

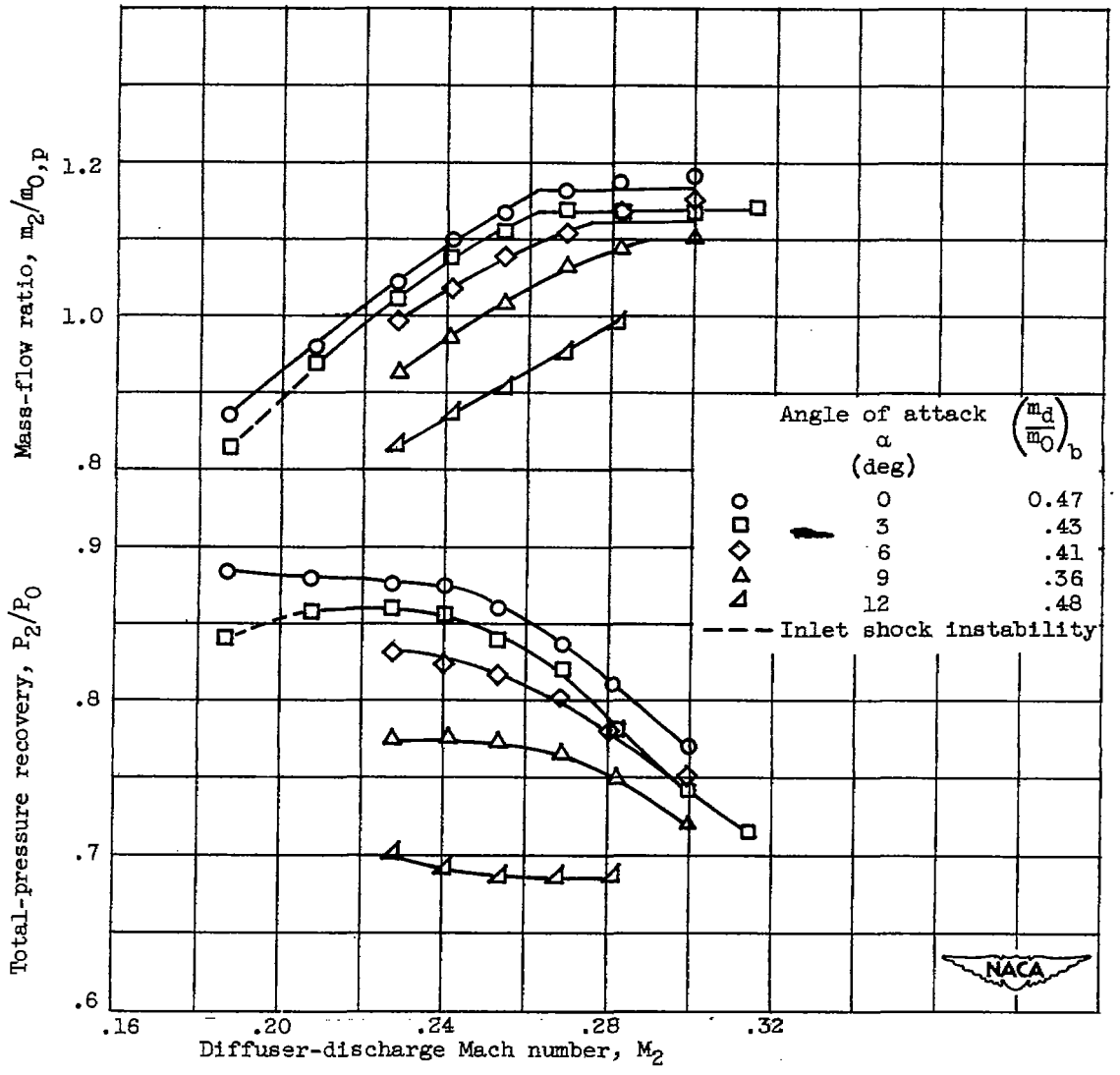

(b) Splitter plate with sweptback leading edge.

Figure 19. - Concluded. Variation of inlet performance with diffuser-discharge Mach number at various angles of attack for redesigned inlet at flight Mach number of 2.0. Forward or flight Mach number = 2.0 cone position.

[redacted]

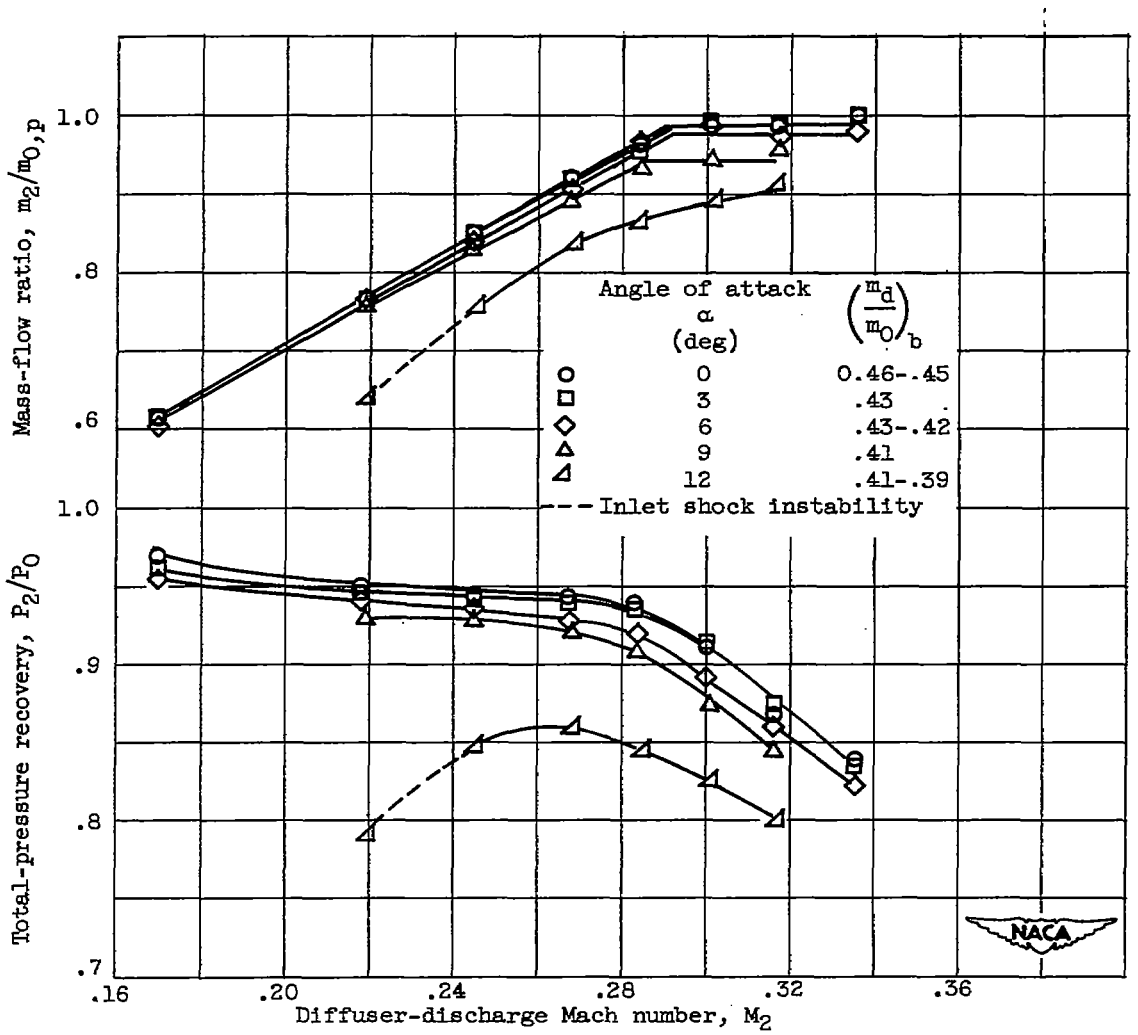

Figure 20. - Variation of inlet performance with diffuser-discharge Mach number at various angles of attack for redesigned inlet with straight leading-edge splitter plate at flight Mach number of 1.5. Aft or flight Mach number = 1.5 cone position.

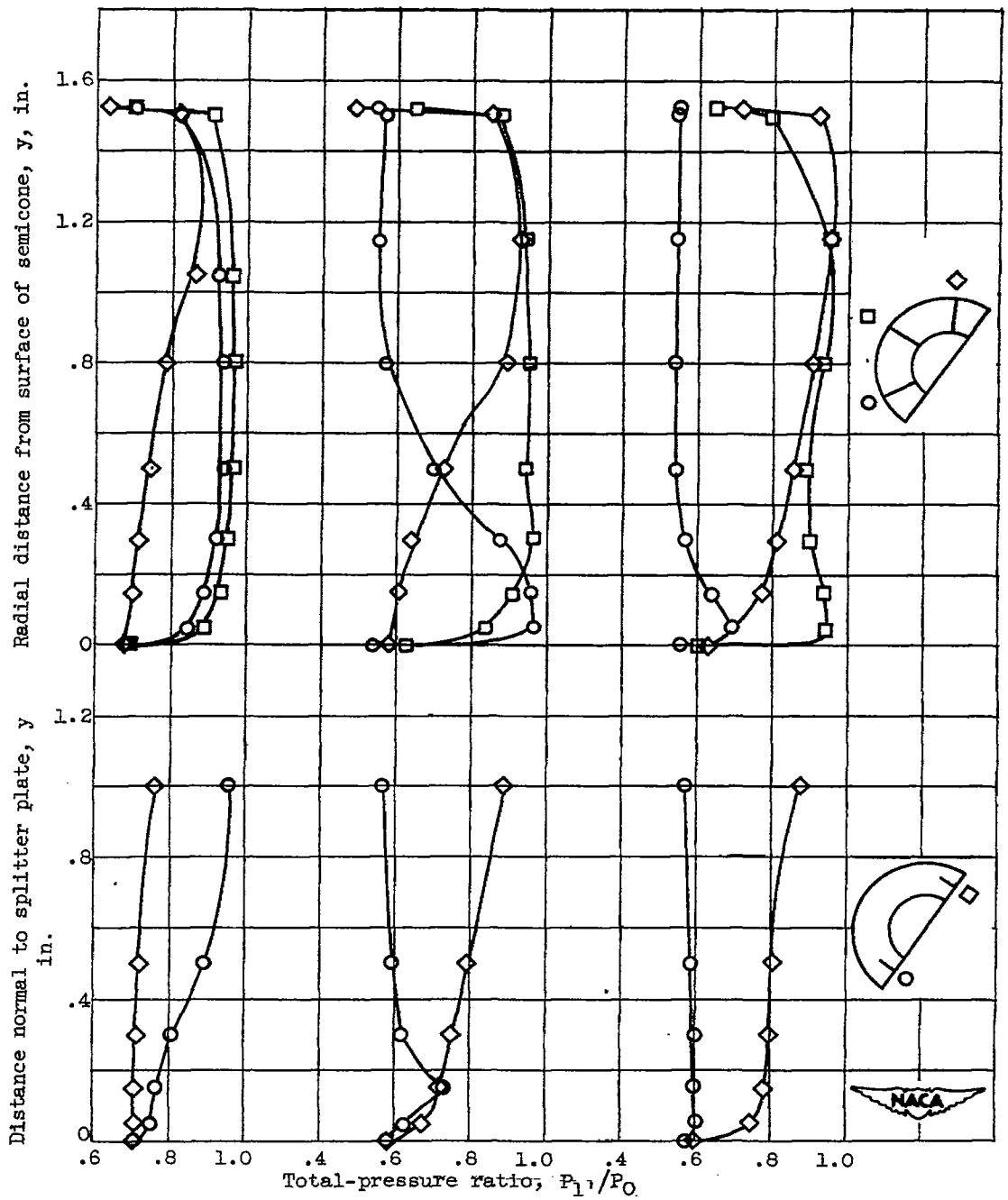

(a) Forward cone position. Flight Mach number, 2.0.

Figure 21. - Starboard inlet total-pressure ratio rake profiles for various angles of attack α and diffuser-discharge Mach numbers M_2.

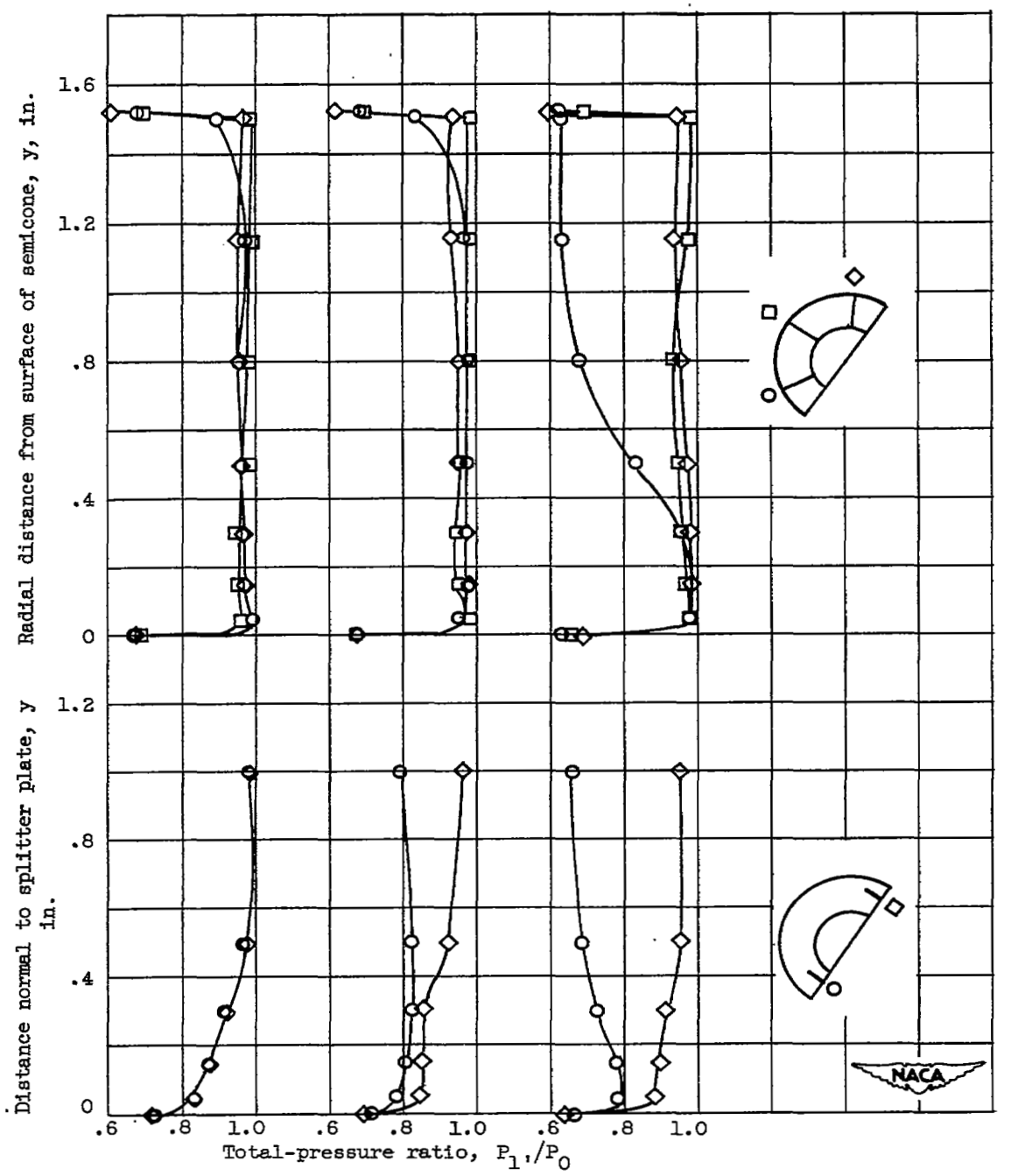

$\alpha = 0^\circ$	$\alpha = 9^\circ$	$\alpha = 12^\circ$
$M_2 = 0.284$	$M_2 = 0.284$	$M_2 = 0.284$

(b) Aft cone position. Flight Mach number, 1.5.

Figure 21. - Concluded. Starboard inlet total-pressure ratio rake profiles for various angles of attack α and diffuser-discharge Mach numbers M_2.

[redacted]

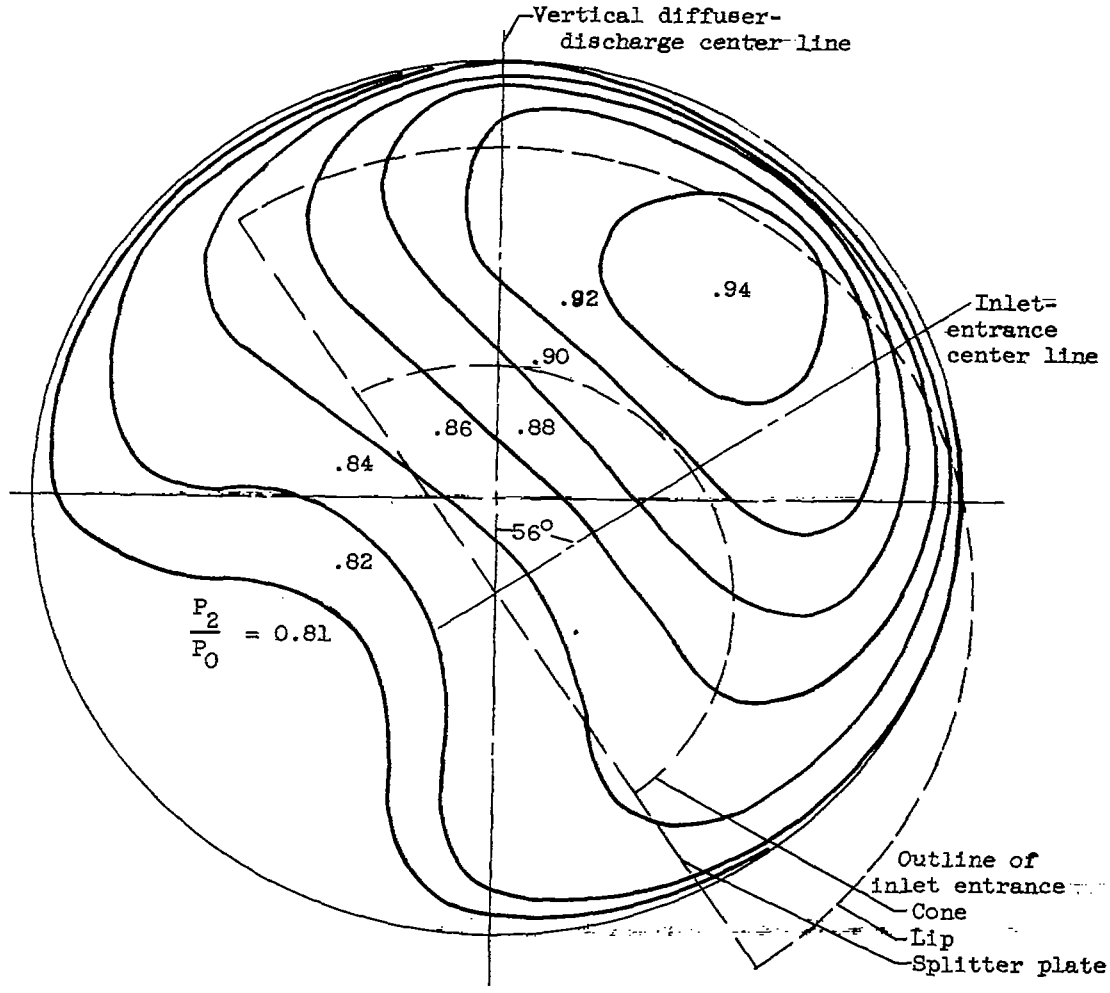

(a) Angle of attack, 0°; pressure recovery, 0.855.

Figure 22. - Diffuser-discharge total-pressure contours for redesigned inlet with straight splitter plate. View in plane normal to angle-of-attack axis looking aft. Flight Mach number, 2.0; diffuser-discharge Mach number, 0.254. Forward cone position.

[redacted]

2507

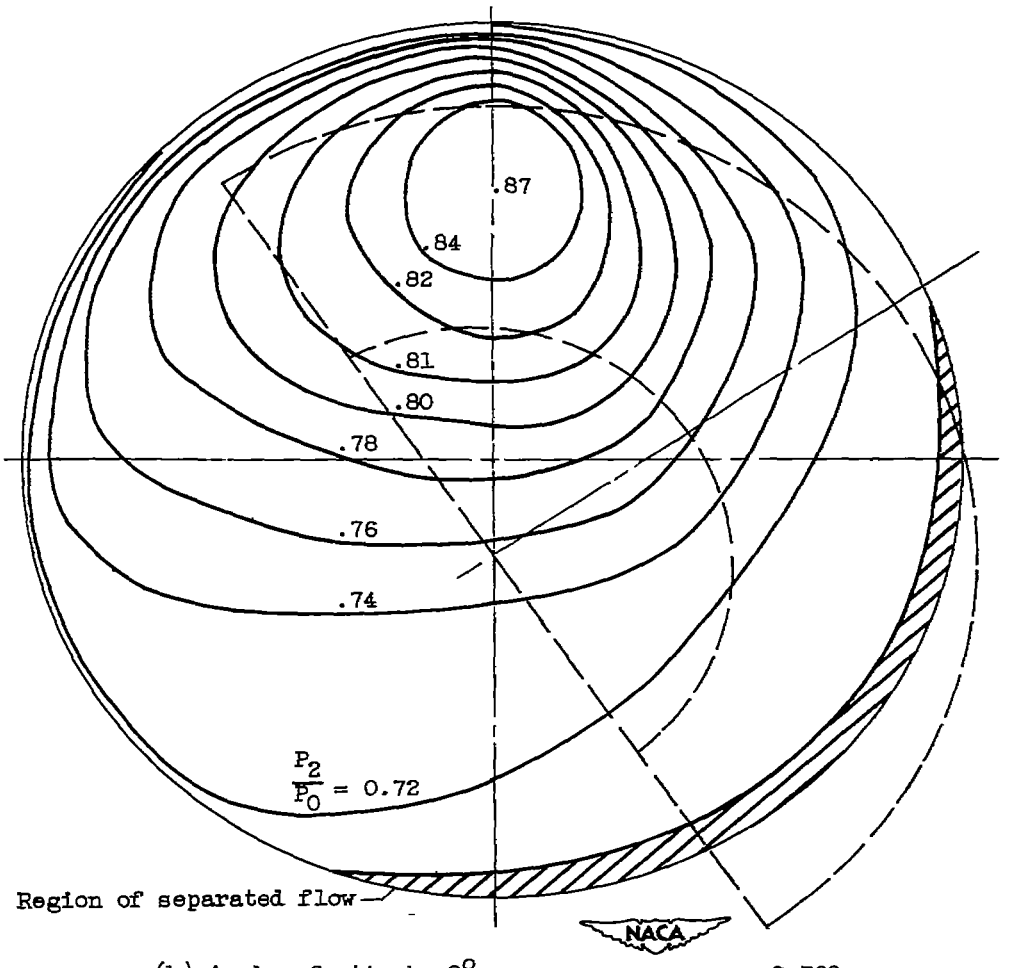

(b) Angle of attack, 9°; pressure recovery, 0.760.

Figure 22. - Continued. Diffuser-discharge total-pressure contours for redesigned inlet with straight splitter plate. View in plane normal to angle-of-attack axis looking aft. Flight Mach number, 2.0; diffuser-discharge Mach number, 0.254. Forward cone position.

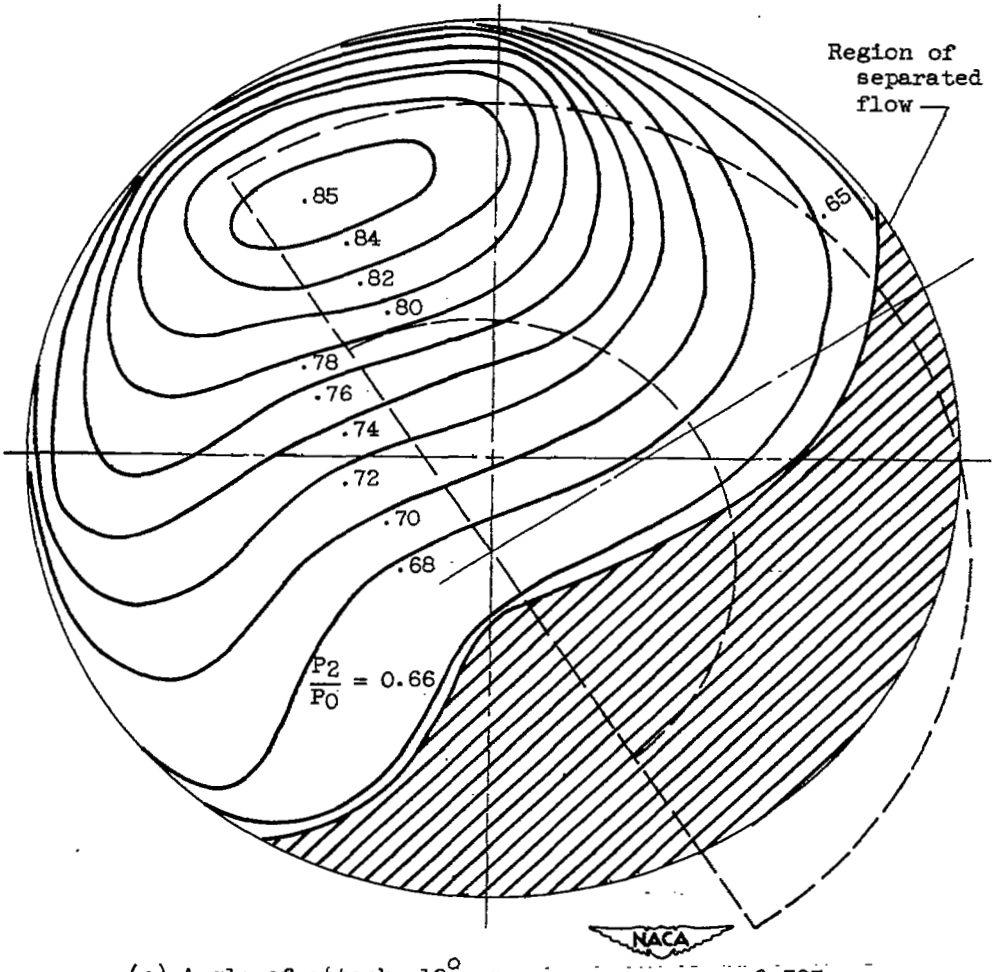

(c) Angle of attack, 12°; pressure recovery, 0.707.

Figure 22. - Concluded. Diffuser-discharge total-pressure contours for redesigned inlet with straight splitter plate. View in plane normal to angle-of-attack axis looking aft. Flight Mach number, 2.0; diffuser-discharge Mach number, 0.254. Forward cone position.

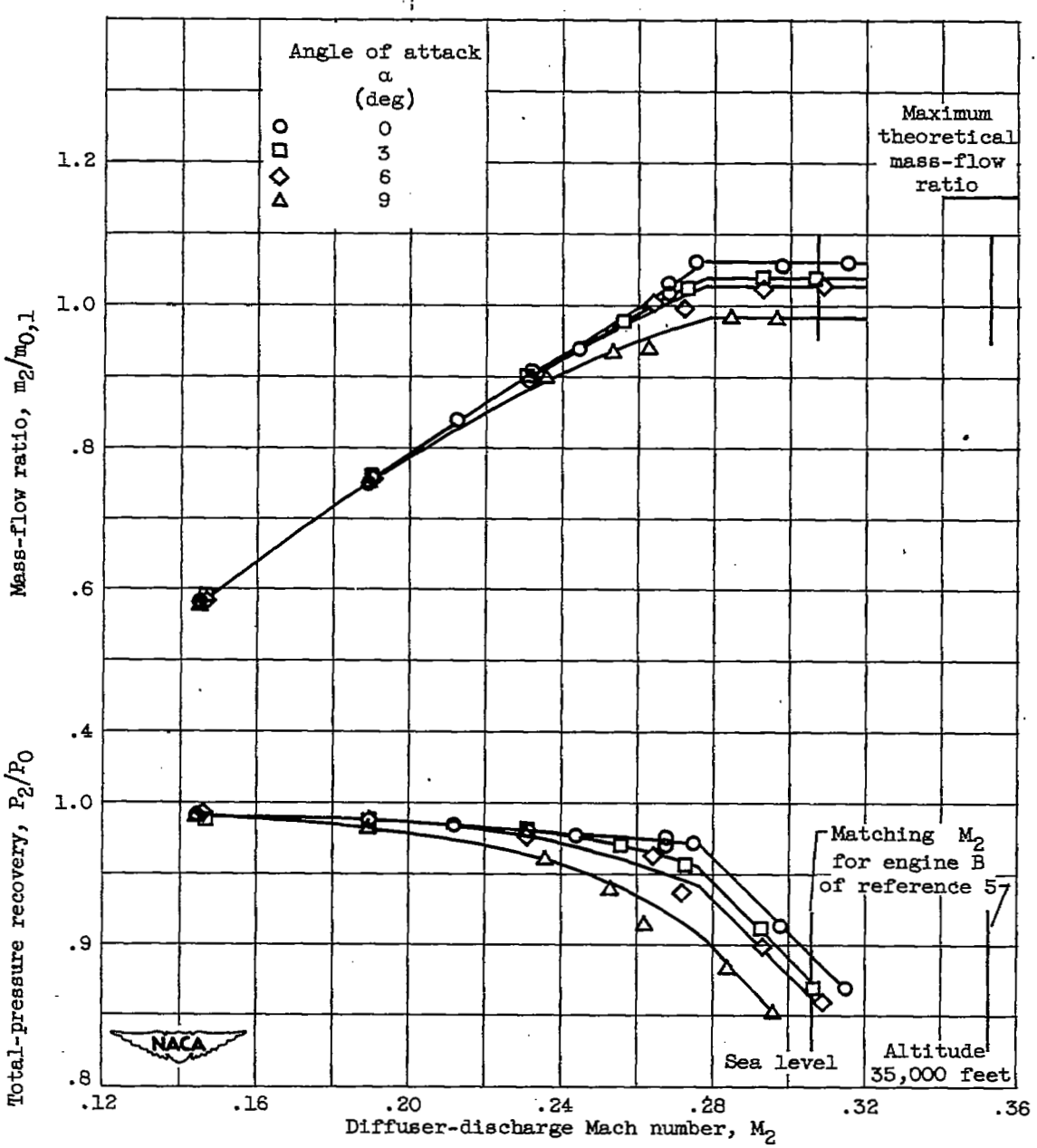

Figure 23. - Variation of inlet performance with diffuser-discharge Mach number at various angles of attack for redesigned inlet with straight leading-edge splitter plate at flight Mach number of 0.63. Aft or flight Mach number = 1.5 cone position. Boundary-layer-duct flow, maximum.

[redacted]

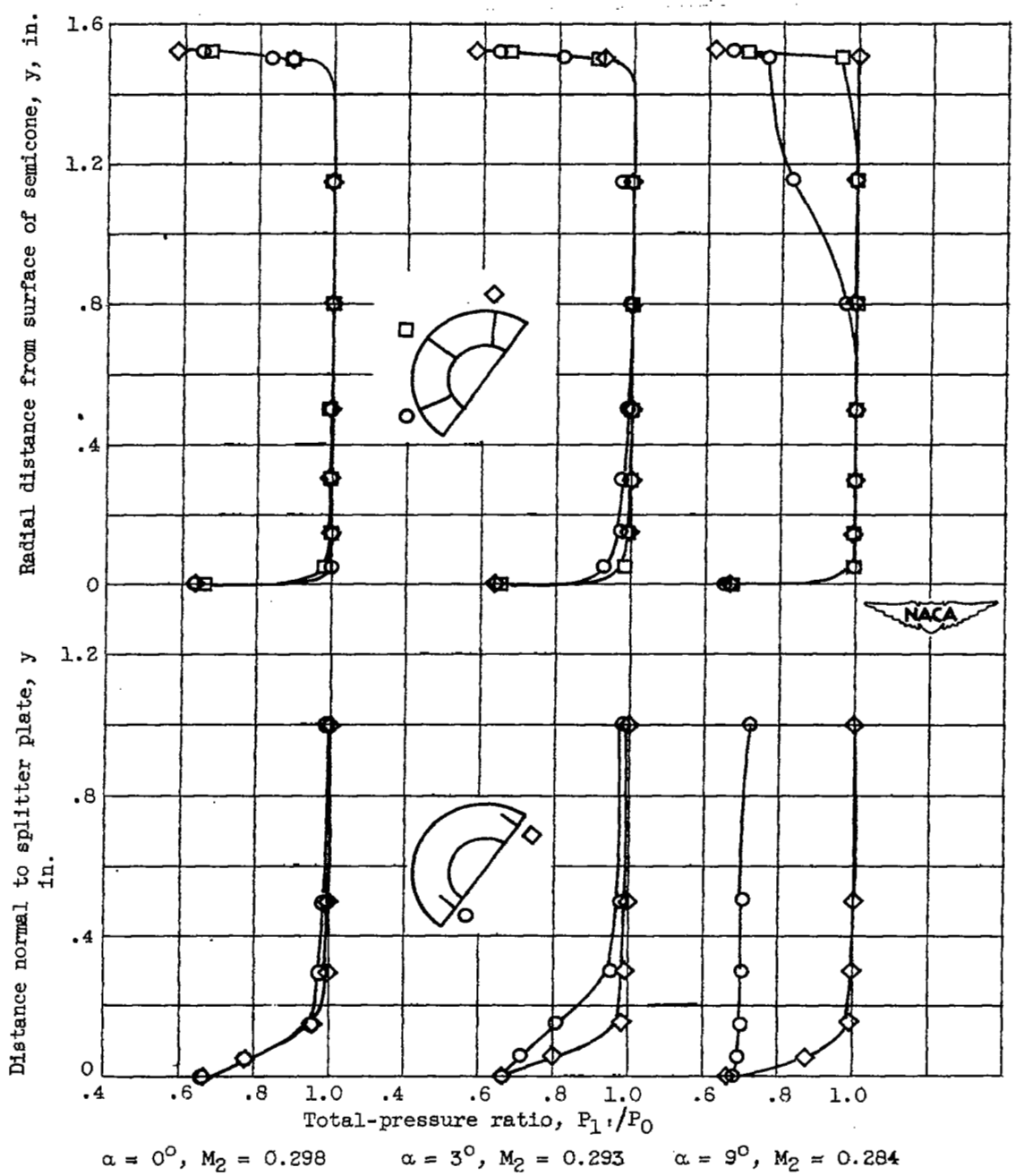

Figure 24. - Starboard inlet total-pressure ratio rake profiles for various angles of attack α and diffuser-discharge Mach numbers M_2. Aft cone position. Flight Mach number, 0.63.

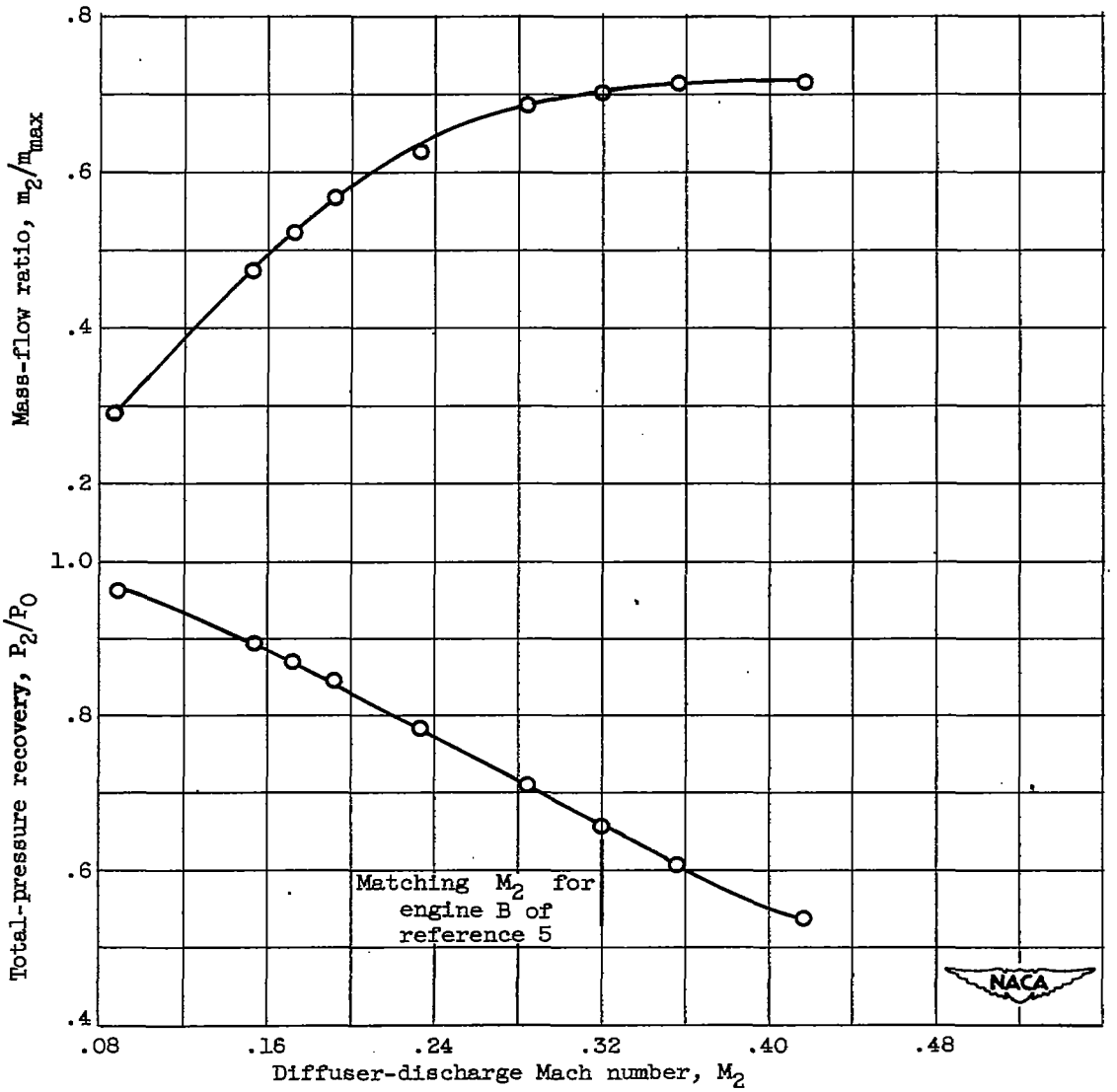

Figure 25. - Variation of inlet performance with diffuser-discharge Mach number at zero flight Mach number for redesigned inlet. Aft or flight Mach number ≈ 1.5 cone position.

[redacted]